INFORMATION TO USERS

This manuscript has been reproduced from the microfilm master. UMI films the text directly from the original or copy submitted. Thus, some thesis and dissertation copies are in typewriter face, while others may be from any type of computer printer.

The quality of this reproduction is dependent upon the quality of the copy submitted. Broken or indistinct print, colored or poor quality illustrations and photographs, print bleedthrough, substandard margins, and improper alignment can adversely affect reproduction.

In the unlikely event that the author did not send UMI a complete manuscript and there are missing pages, these will be noted. Also, if unauthorized copyright material had to be removed, a note will indicate the deletion.

Oversize materials (e.g., maps, drawings, charts) are reproduced by sectioning the original, beginning at the upper left-hand corner and continuing from left to right in equal sections with small overlaps.

Photographs included in the original manuscript have been reproduced xerographically in this copy. Higher quality 6" x 9" black and white photographic prints are available for any photographs or illustrations appearing in this copy for an additional charge. Contact UMI directly to order.

Bell & Howell Information and Learning
300 North Zeeb Road, Ann Arbor, MI 48106-1346 USA
800-521-0600

UMI®

Improved Nonlinear Modeling and Control of Electro-Hydraulic Systems

A Thesis Presented

by

Bora ERYILMAZ

to

The Department of Mechanical, Industrial,
and Manufacturing Engineering

in partial fulfillment of the requirements
for the degree of

Doctor of Philosophy

in the field of

Mechanical Engineering

Northeastern University
Boston, Massachusetts

August 2000

UMI Number: 9988498

Bell & Howell Information and Learning Company
300 North Zeeb Road
P.O. Box 1346
Ann Arbor, MI 48106-1346

To my parents

Özden and Sabri Eryilmaz

and my best friends

Bircan, Kurtan, Mustafa and Yeşim

Abstract

Electrohydraulic systems promise unique application opportunities and high performance, unmatched by other drive technologies. Typical applications include robotic manipulators, motion simulators, injection molding, and material testing machines. However, the continuing success of electrohydraulic systems over competing drive technologies is contingent upon surpassing traditional performance levels, both in terms of physical measures such as motion precision and in terms of economic measures such as product cost. Improving these measures requires a closer look at the hydraulic system dynamics (models) and an evaluation of advanced control techniques as they apply to hydraulic systems.

The need for a better understanding of hydraulic system dynamics directed part of our research to obtaining detailed models of active hydraulic system components. Specifically, we have developed detailed nonlinear models of orifice and leakage flows in proportional and servo valves. For controls, we have investigated the application of singular perturbation control to hydraulic systems.

The valve model provided a concise description of orifice flows for a wide range of proportional valves with various spool types. The leakage model resulted in a better characterization of leakage flow within servovalves, especially around null spool position where leakage flow is likely to dominate. The singular perturbation control design not only provided improved tracking performance, but it also ensured robustness against uncertain and time-varying fluid bulk modulus, an effect present in all hydraulic systems.

The results reported in this thesis make available new tools to analyze and improve the performance of electrohydraulic control systems. Model-based control design may benefit from the new models, since a better description of hydraulic system dynamics is now available. The nonlinear proportional valve model along with a nonlinear controller may allow the use of less expensive and less precise valves in active vehicle vibration isolation, where the valve cost is a major deterrent for commercial applications. In hydraulic material testing machines, the leakage model may be used to improve the precision motion performance in some tests such as creep loading, where the valve spool mostly resides within the null region

with relatively large leakage flows. The singular perturbation control design will provide robust performance in applications. where the bulk modulus varies over time.

Acknowledgements

I would like to thank the Instron Corporation and Barry Controls for their financial and hardware support, and the Moog Inc. for providing various experimental data.

I would also like to thank Andrew Beard and Mark Peretti of (formerly) Barry Controls, and Murray Nicholson, Yahya Gharagozlou, Fred Lehman, and Paul Biasi of Instron Corporation for their help and guidance during my research.

Most important, the dedication of my advisor Prof. Bruce H. Wilson is greatly appreciated. This work has been made possible by his constant support and guidance since the first day I have been his student.

Finally, I would like to acknowledge the support of many professors in the Department of Mechanical Engineering and the Department of Mathematics at Northeastern University. They have greatly influenced my vision and appreciation of scientific knowledge.

BORA ERYILMAZ

Northeastern University

August 2000

Contents

List of Figures

Nomenclature

A_1	piston end cylinder area	m^2
A_2	rod end cylinder area	m^2
A_p	cylinder area	m^2
C_d	valve discharge coefficient	
f	signal frequency	Hz
F	piston force	N
F_f	friction force	N
F_{hyd}	hydraulic force	N
$k_{iR(S)}$	port i return (supply) side leakage coeff.	
K_c	valve pressure gain	m^4s/kg
$K_{iR(S)}$	port i return (supply) side flow gain	$m^{5/2}/kg^{1/2}$
K_q	critical center valve flow gain	m^2/s
L	valve port opening	m
P_i	port i pressure	N/m^2
$P_{iR(S)}$	port i return (supply) side pressure	N/m^2
P_L	load pressure	N/m^2
$P_{R(S)}$	return (supply) pressure	N/m^2
P_V	valve pressure drop	N/m^2
Q_i	port i total flow rate	m^3/s
$Q_{iR(S)}$	port i return (supply) side flow rate	m^3/s
Q_{ip}	leakage flow rate	m^3/s

Q_L	load flow	m^3/s
$Q_{R(S)}$	total return (supply) flow rate	m^3/s
R_{ip}	cylinder leakage coefficient	m^4s/kg
S	piston stroke	m
v_p	hydraulic piston velocity	m/s
V_{10}	initial volume (piston end)	m^3
V_{20}	initial volume (rod end)	m^3
V_1	chamber volume (piston end)	m^3
V_2	chamber volume (rod end)	m^3
V_t	total cylinder volume	m^3
w	valve area gradient	m
x_0	equivalent orifice opening	m
x_p	hydraulic piston position	m
x_v, x	valve spool position	m
β	fluid bulk modulus	N/m^2
$\varepsilon_{iR(S)}$	port i spool lapping parameters	m
ε_i	spool lapping parameters	m
ρ	fluid mass density	kg/m^3
ω	signal frequency	rad/s
ω_h	hydraulic natural frequency	rad/s
μ	coulomb friction	N
ζ_h	hydraulic damping coeff.	-

Chapter 1

Background and Literature Review

1.1 Description of the Problem

Hydraulic actuators are used in applications that require fast motion and large actuation forces. Typical areas of application include industrial robots, material handling machines, active suspensions, motion simulators, and injection molding machines. Indeed, hydraulic actuators are often the only viable alternative for these applications, because other actuators, such as electric motors, usually lack the necessary power, size, and speed. Despite this extensive application, actively-controlled hydraulic systems do not fully realize their potential due to, among other factors, difficulties in modeling and controlling their highly nonlinear characteristics.

The mathematical models for hydraulic system components have been developed by early researchers and are available in standard books on the subject [38, 37, 10, 53]. Among these components, flow control valves are the most important because they most directly affect the dynamic properties of the system. Typical flow control valves include servovalves or proportional valves.

The proportional and servovalves are used regulate the oil flow rates, and thereby the motion, of a hydraulic system. Due to the nature of orifice flow inside the valve body, these valves are the major source of nonlinearities in hydraulic systems. The nonlinear

flow property is present regardless how precise the valve body and the enclosed spool are produced. In addition, most valves exhibit further nonlinearities such as deadzone due to valve spool overlap, hysteresis due to magnetic properties of the solenoid coil driver, friction, and nonlinear flow forces. Without the proper analysis and design tools, the benefits of hydraulic servosystems may be overshadowed by the problems in dealing with such complex nonlinear systems.

Most hydraulic component models have been developed for subsequent application of linear control design tools; they are therefore simple and linear. In precision motion control applications, however, the various nonlinearities mentioned cannot be ignored because they can greatly degrade the system performance. Furthermore, linear control theory cannot adequately cope with nonlinearities such as deadzone or friction. Hence for such applications, linear controllers are simply not capable of providing high performance. This is especially true when economic considerations drive the use of less expensive and less precise components. In order to fully realize the capabilities of hydraulic systems, more complete models of hydraulic systems components must be developed, and these models must be incorporated into the design of advanced controllers.

In the following sections, we first review the available literature on modeling the dynamics of hydraulic systems and various nonlinear control techniques as they relate to electrohydraulic system applications. A brief description of our research and the underlying motivations are presented next. We conclude with a discussion of the implications of our new results.

1.2 Literature Review

As a precursor to developing improved analysis and control tools for electrohydraulic systems, we surveyed the available results on modeling hydraulic control valves and the relevant techniques in control theory. In the next sections, we first review the literature on modeling hydraulic flow control valves. Specifically, we present the results on modeling of various flow nonlinearities introduced by valve properties. Next, we review the literature on nonlinear

control techniques relevant to the control of electrohydraulic systems. Adaptive nonlinear and singular perturbation control techniques are discussed in more detail, since they are readily applicable to hydraulic systems. Finally, we address some of the gaps in the current literature on modeling and control of electrohydraulic systems and point to possible research opportunities in these areas.

1.2.1 Modeling and Analysis of Electrohydraulic Systems

In this section, we review some of the literature available on modeling hydraulic flow control valves, in particular proportional and servovalves. The focus is on the modeling of various flow nonlinearities, introduced by orifice flow, valve leakage, and valve geometry.

The nonlinear response found in control valves results in nonlinear behavior of the hydraulic systems employing these valves. Furthermore, when configured into a hydraulic system, components such as pumps, accumulators, hoses, valves, and cylinders, each contribute to the overall dynamic response. As the components are coupled, the modeling task becomes increasingly difficult. In this respect, a systematic approach to modeling hydraulic system dynamics proves to be useful [11, 17].

Among the many hydraulic systems components, the control valves such as proportional and servovalves are the most important. Their dynamics determine the basic response and stability characteristics of hydraulic systems, since they are often the only actively controlled components in the system. Models of various configurations of control valves are available in [28, 54], and hysteresis modeling in proportional valves is provided in [52]. These models provide some understanding of complex interactions between electrical, mechanical, and fluid aspects of hydraulic control valves. But they don't describe the nonlinear flow properties within various flow regimes resulting from geometric valve properties.

Hydraulic valves exhibit various nonlinear behaviors in the form of both smooth and nonsmooth relations among various system variables. The fundamental smooth nonlinearity in hydraulic valve models is the square-root term in the orifice flow equations, which is always present. This term is essentially a nonlinear input gain, which varies as a function of

chamber pressures in a cylinder attached to the valve. Non-smooth nonlinearities arise from geometric imperfections of the valve and its spool. These nonlinearities manifest themselves as deadzones in overlapped valves and as piecewise-linear nonlinearities in underlapped valves. If ignored during controller design, hydraulic system nonlinearities may greatly degrade or even destabilize the hydraulic system performance. In this respect, the analysis of hydraulic system stability is of particular importance, as discussed in [55, 36].

The leakage flow between a servovalve spool and valve body is another key consideration in applications involving precision positioning. The valve leakage results in a nonlinear flow relation in the vicinity of neutral spool position. An ideal servovalve has perfect geometry, so that leakage flows are zero. In this case, the theoretical orifice equation holds over the whole range of spool travel [38]. But for actual servovalves, this relation only holds outside the null region. Experimentation and analysis indicate that, at small spool displacements, the leakage flow is much larger than the orifice flow. Most servohydraulic designs are based on the ideal orifice relation, e.g. [39, 45], applied through the entire range of spool motion. The use of such models for design appears somewhat questionable, given the applicability of ideal relations only outside of the null region and the dominance of leakage flow within the null region.

Although models of leakage flow in servovalves are available in the literature, these models impose limitations on the spool geometry and valve properties. The leakage flow model developed in [20] assumes a small and symmetric overlap between the spool lands and the valve control ports. However, this model is only valid for a small positive spool displacement limited to approximately two percent of maximum spool travel. Furthermore, the model predicts non-smooth flow rate curves for small orifice openings, due to the non-smooth transition from the assumed laminar leakage to turbulent orifice flow. The model developed in [18] circumvents this problem and provides smooth transition from leakage to orifice flow. This model approximates the leakage flow path in a servovalve as a short annulus of fine clearance and employs the laminar flow model developed in [19]. The resulting model is, however, too complex to be used for practical design of nonlinear controllers to improve

hydraulic system performance. A simpler and easy-to-parameterize model of leakage flow would be more valuable for analysis and control design.

1.2.2 Control of Electrohydraulic Systems

In this section, we review some of the literature available on nonlinear control techniques as they apply to the control of electrohydraulic systems.

Various control techniques developed in recent decades such as adaptive and singular perturbation control, as well as Lyapunov based nonlinear control are especially relevant for the improved control of hydraulic systems. These techniques require better models of hydraulic system dynamics to cope with ever increasing demand for higher performance with no additional cost. Indeed, the only apparent way to improve the performance without using expensive components is to incorporate previously neglected dynamics such as nonlinearities and leakage into the controller synthesis process.

A common approach to incorporate the square-root nonlinearity into the controller design process is to invert this term by measuring the cylinder chamber pressures. Following this approach, Sohl and Bobrow [44, 45] applied Lyapunov techniques to design nonlinear controllers for position and force control of a hydraulic system. However, they assumed constant system parameters, identified using an off-line least-squares method. Nonlinear force control is treated by Alleyne [6], and its limitations are discussed in [9, 21]. Adaptive control of hydraulic systems with unknown or time-varying parameters is discussed in [12, 40]. However in [40], only one parameter group, treated as a single parameter, is assumed unknown, even though some of the parameters in the group appear elsewhere in the system model equations. Sliding mode control of a hydraulic suspension system is developed in [8]. In [26], sliding mode control is applied to control a solenoid-driven proportional valve. However, the control focuses on the position control of the valve spool without analyzing its effect on any attached hydraulic system configuration. The feedback linearization approach is applied to hydraulic systems in [27], where a differentiable (diffeomorphic) transformation is used to linearize the input-output behavior of the hydraulic system [31].

Although square-root nonlinearity in hydraulic systems is relatively easily compensated, non-smooth nonlinearities such as deadzone, hysteresis, and friction are much more difficult to contend with via control. The emerging area in control theory of nonlinear control of systems with non-smooth nonlinearities addresses these effects. One approach to this problem is the adaptive inverse control of nonlinear systems first introduced by Recker [41] and later developed by Tao and Kokotović in [46, 47, 48, 49]. Another approach is the variable structure or sliding mode control of systems with non-smooth nonlinearities [29]. These approaches appear applicable to the design of hydraulic control systems, but the existing theory may be difficult and costly to implement in commercial hardware. Some preliminary implementation results reported in [16] point to the limited success of the theories developed in [49] to control real systems with non-smooth nonlinearities. More important, as indicated in [41], further work is required for adaptive compensation of multiple piecewise-linear non-smooth nonlinearities, which are more relevant in the case of less expensive hydraulic proportional valves.

The inherent slow and fast dynamics is another characteristic feature of hydraulic systems. In general, the mechanical dynamics, which are characterized by force-velocity and force-displacement relations, will be considerably slower than the fluid dynamics of pressure transients. The resulting two-time-scale behavior fits into the framework of singular perturbation theory. Although singular perturbations have been discussed in the framework of control theory [33, 34, 35], applications to hydraulic systems are few and limited in scope. In [32], Kim applies singular perturbation analysis to a hydraulic active suspension system to justify the model order reduction of a servovalve electrical subsystem. In [14], d'Andréa Novel et al. design stabilizing and tracking controllers for a hydraulic robot using singular perturbations.

Controllers for hydraulic systems are often designed using a simplified model where some of the fast dynamics of the system are ignored. This ad-hoc approach stems from mathematical convenience without rigorous justification. A more detailed analytical study would help develop and evaluate context-dependent models of hydraulic systems. By bringing singular

perturbation modeling and analysis techniques into the realm of hydraulic systems, it is possible to match model complexity with the control requirements, thus providing analytical justification to model simplification. Alternatively, singular perturbation control theory can be used for designing efficient "composite" controllers by decomposing the feedback design problem into two design subproblems for the slow and fast dynamics [13, 42, 43, 30]. The two designs are then combined to give a design for the full system.

1.2.3 Need for Further Research

Although various models of hydraulic flow control valves have been developed by researchers, most of these models are not intended to be used for subsequent control design. Accordingly, the model parameters are difficult to measure or characterize. On-line identification of these parameters for adaptive control purposes may also require expensive sensors and heavy computations. Therefore,

> Simple-to-characterize yet precise models of nonlinear valve flow dynamics would be a valuable tool for the control designer.

At present, most of the electrohydraulic control systems use conventional PID (proportional, integral, and derivative) controllers. Historically, these controllers provided satisfactory performance because of the inherently nice properties of hydraulic systems, such as large bandwidth, high gain, and high stiffness. However, the requirements of ever higher performance and smaller product size limit the performance of hydraulic systems attainable using conventional controllers. In such cases, these controllers cannot provide satisfactory performance and robustness against parameter variations and flow nonlinearities. Hence,

> New control techniques should be developed, or existing approaches should be adapted to improve the performance of hydraulic control systems.

1.3 Research Summary

Considering the need for improved modeling and control of hydraulic systems, we focussed part of our research in obtaining detailed models of hydraulic system components, especially, proportional and servovalves [23, 24]. These models provide basic tools for the implementation of various nonlinear control techniques to improve hydraulic system performance, without using expensive components. In particular, model-based control design may benefit from these improved models, since a better description of hydraulic system dynamics is available.

For control, we investigated the applicability of singular perturbation control techniques to hydraulic systems, with encouraging preliminary simulation results [22]. The resulting controller not only provides improved tracking performance, it also ensures robustness against uncertain and slowly varying bulk modulus.

Although model-based control techniques will benefit from the use of our detailed models of valve dynamics, improved performance requires a priori knowledge of system configuration and properties. On the other hand, robust control techniques such as singular perturbation control are less sensitive to variations in system properties, and may provide better performance for a wider range of system configurations. For highly nonlinear systems such as hydraulic systems, robustness to parameter variations should be ensured for acceptable performance in real-world applications. Summaries of *our dual approach of better modeling and better control* to improve the performance of electrohydraulic systems follow.

1.3.1 Proportional Valve Modeling

Developments in nonlinear control theory facilitate design of controllers for systems having non-smooth nonlinearities in their dynamics. Hydraulic systems that use inexpensive proportional valves are examples of such systems, where non-smooth nonlinearities arise due to valve geometry and spool imperfections. However, without a proper valve model, nonlinear analysis and control of these hydraulic systems is not possible. In Chapter 2, we develop nonlinear equations for a generic proportional valve model, which we have used to

obtain simplified flow rate expressions under generally accepted assumptions [23]. These equations relate a set of geometric spool properties and physical model variables to the flow rate through the valve ports. The development focuses on obtaining a *single set* of flow rate equations for the cases of critical center, overlapped, and underlapped proportional valves. The proportional valve model equations are useful for system simulation and for nonlinear controller design. In Chapter 3, we analyze the accuracy of this generic proportional valve model. The accuracy of the model is determined through a non-dimensional analysis approach, and the results hold for any similar system. Hence, given a set of hydraulic system parameters, the engineer may determine a priori whether the valve model will provide an accurate representation of the valve dynamics for subsequent analysis and control design.

1.3.2 Modeling Leakage Flow in Servovalves

In our subsequent research [24], we considered flow, in particular, leakage flow, between a servovalve spool and valve body. Although often ignored, experimentation and analysis indicate that at small spool displacements this flow is much larger than orifice flow. In precision positioning applications, where the servovalve generally operates within the null region, leakage flow may severely degrade the performance of conventional servohydraulic designs based on an ideal orifice relation. Hence, servovalve models for such applications should include leakage flow. In Chapter 4, we develop a model for leakage flow in a servovalve. This has been achieved by reviewing experimental leakage flow data and identifying a simple mathematical form that *(1)* makes physical sense and *(2)* can replicate experimental data. The resulting model accurately captures leakage behavior, which is modeled as turbulent flow with a flow area inversely proportional to the overlap between the spool land and valve orifices. When combined with orifice relations, the model extends the accuracy and region of applicability of existing servovalve models. Furthermore, the leakage model is easily parameterized, an important feature for controller design and adaptive methods.

1.3.3 Singular Perturbation Control of Hydraulic Systems

Tracking control for hydraulic systems is a key system requirement, as these devices must often follow prescribed motions. Tracking control of hydraulic systems has been approached using both linear and nonlinear control laws. The latter provides improved performance, but at the expense of additional sensors. Further, the control laws often employ hydraulic fluid bulk modulus –a difficult-to-characterize quantity– as a parameter. In Chapter 5, we provide a new control design procedure to overcome these difficulties. The resulting controller requires no additional sensors and the hydraulic system is robust to variations in the bulk modulus [22]. A dual approach of singular perturbation theory and Lyapunov techniques forms the basis of the procedure. For the cases of a small-amplitude sinusoidal input and a large-amplitude polynomial input, a candidate system achieved good tracking performance and exhibited outstanding robustness. The ability to accomplish good tracking in a robust manner with no additional sensors provides advantages over other nonlinear tracking algorithms, where the effective bulk modulus is treated as a known and fixed parameter [40, 45].

1.3.4 Future Research

The work reported here provides a good foundation for further research in improving the performance of electrohydraulic systems. In particular, new research should seek further developments in incorporating the proportional and servo valve models developed here with various nonlinear control techniques and analyze the robustness of these techniques to parameter variations.

This thesis also provides new tools to analyze and improve the performance of electrohydraulic control systems. Possible applications of these results include the use of less expensive (and non-smooth nonlinear) proportional valves together with a nonlinear controller in active vehicle vibration isolation systems, where the valve cost is a major deterrent for commercial applications. In hydraulic material testing machines, the use of the leakage model may be used to improve the precision motion performance in some tests such as creep

loading, where the valve spool mostly resides within the null region with relatively large leakage flows.

Chapter 2

A Unified Model of a Proportional Valve

2.1 Introduction

Hydraulic systems are often employed in high performance applications that require fast response and high power. These applications include high bandwidth control of position and force [12, 44], active vibration isolation in vehicles [8], and control of multi-axis robotic manipulators [51]. The hydraulic actuator, usually a cylinder, provides the motion of the load attached to the hydraulic system. A control valve meters the fluid into and out of the actuator as a spool traverses within the valve body. The control valve is either a servovalve or a proportional valve. The less expensive proportional valve consists of a solenoid that is directly attached to the spool, and the spool displacement is, in principle, proportional to the input current. The performance of hydraulic systems strongly depends on the control valve and spool geometry and their manufacturing tolerances. The manufacturing precision distinguishes proportional valves from servovalves, in terms of both performance and cost.

In hydraulic control applications, proportional valves offer various advantages over servovalves. Proportional valves are much less expensive. They are more suitable for industrial environments because they are less prone to malfunction due to fluid contamination. In ad-

dition, since proportional valves do not contain sensitive, precision components, they are easier to handle and service. However, these advantages are somewhat offset by nonlinear response characteristics.

Since proportional valves have less precise manufacturing tolerances, they may suffer from performance degradation. The larger tolerances on spool geometry result in response nonlinearities, especially in the vicinity of neutral spool position. Proportional valves lack the smooth flow properties of "critical center" valves, a condition closely approximated by servovalves at the expense of high machining cost. Small changes in spool geometry (in terms of lapping) may have large effects on the hydraulic system dynamics. For example, a "closed center" (overlapped) spool may result in steady state error because of its deadzone characteristics in the flow gain [38]. An "open center" (underlapped) spool, on the other hand, may raise stability concerns due to the increased flow gain near neutral spool position. Hence, a critical center valve model is not sufficient for designing hydraulic control systems using proportional valves. A more comprehensive model of proportional valves is necessary in designing and analyzing hydraulic systems.

Various researchers have developed mathematical models of proportional control valves [38, 53]. However, these works usually assume a critical center valve spool whose motion is restricted to the vicinity of the neutral position for subsequent linearized analysis. Modeling and analysis of underlapped valves are briefly discussed under the restrictive assumption that the spool moves within the underlap region [38]. The overlapped valve models are, in general, ignored from the discussion. More general valve models have also been developed, however, they usually apply to expensive critical center servovalves [54, 55] or various configurations of flow control valves [28]. A generic proportional valve model applicable under all operating regimes and for all types of spool lapping is lacking.

Without the proper model, nonlinear analysis of hydraulic system performance is not possible. As a number of nonlinear control strategies have been developed in the last decade [47, 49], the availability of a general nonlinear model of a proportional valve would increase the likelihood that the former could be applied to the latter. In this chapter, we

develop a nonlinear mathematical model for a generic proportional control valve. This model relates a set of geometric spool properties and physical variables to the flow rate through the valve ports. The development focuses on obtaining a *single set* of flow rate equations for the cases of critical center, overlapped, and underlapped proportional valves. The flow rate is expressed as a continuous but nonlinear function of spool lapping parameters, as well as other conventional parameters. We derive simplified flow rate equations under certain generally accepted assumptions (such as equal cylinder chamber volumes and incompressible fluid), while keeping nonlinearities due to spool geometry. The variation of the flow gain and uncertainty bounds of the flow rates as a function of valve and lapping parameters are also analyzed.

This chapter is organized as follows. We first develop the orifice flow equation for a flexible orifice model that describes various nonlinear effects. The orifice equation forms the basis of the hydraulic proportional valve model. In a typical hydraulic control application, a hydraulic cylinder serves as the actuator. In the next section, we present the mathematical model for such actuators. The proportional valve equations are then simplified under widely accepted assumptions, and flow properties of these valves as a function of the lapping parameters are analyzed. The chapter closes with a brief discussion of conclusions and future research directions.

2.2 Development of Proportional Valve Model

Many fluid power control applications use a variable orifice for controlling the fluid flow. A sliding element, or spool, has various "lands" that modulate flow. The spool moves in a bore (sleeve) containing ports. The movement of the spool causes each land to vary the area of the corresponding ports exposed to the flow, thereby changing the flow-versus-pressure relationship of the orifices. An underlapped spool has an orifice port opening that is larger than the land; whereas an overlapped spool has an orifice port opening that is smaller than the land.

The variable orifice in Figure 2.1 is the basic element for controlling hydraulic systems. It

has three flow rates associated with the orifice ports (Q_{1S}, Q_{1R}, Q_1). The supply and return

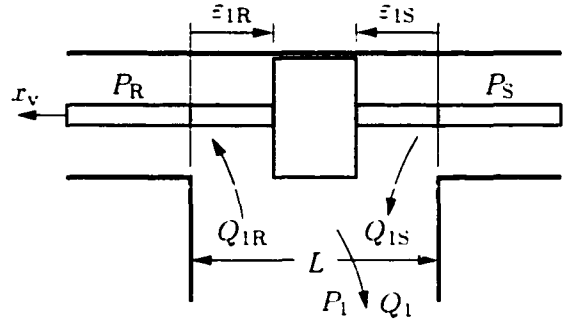

Figure 2.1: Spool valve orifice.

ports connect to the pump and tank lines respectively. The orifice output port provides the regulated flow and usually connects to an actuator such as a hydraulic cylinder. The parameters ε_{1S} and ε_{1R} represent the spool underlap or overlap (at neutral spool position) on the supply and return ports of the orifice, and they can be set independently. With respect to the neutral spool position, *positive* values of these parameters correspond to spool *underlap* (shown in Figure 2.1). Similarly, *negative* parameter values define an *overlapped* spool.

Various simplifying assumptions and valve models are used in applications. Most hydraulic control systems employ critical center valves, where the spool lands perfectly match the valve ports so that $\varepsilon_{1S} = \varepsilon_{1R} = 0$. Typically, the supply pressure, P_S, is larger than the port pressures, (e.g. P_1), and the return (tank) pressure, P_R, is small. This assumption avoids the flow reversal so that the flow is either directed from the supply line to the output port, or from the output port to the return line. To avoid flow saturation and to use linearized analysis, the spool travel is in general restricted so that $|x_v| \ll L$. Under these conditions, the orifice equations simplify to

$$Q = \begin{cases} C_d w \sqrt{2/\rho} \sqrt{P_S - P_1}\, x_v, & x_v \geq 0. \\ -C_d w \sqrt{2/\rho} \sqrt{P_1 - P_R}\, x_v, & x_v < 0. \end{cases}$$

so that only the supply or the return orifice is open at a given time [38].

Although the above assumptions simplify the orifice model, they do not always hold in high performance applications. In hydraulic control systems rapid changes of fluid flow properties are associated with rough disturbance inputs and the motion of large dynamic loads. Under these conditions, various flow anomalies might occur. These include back flow into the supply line ($P_1 > P_S$) or from the tank ($P_1 < P_R$). Further, the spool may not be critically centered, either intentionally or due to manufacturing tolerances. Hence, both the supply and return orifices or none of them may be open at a given time. These considerations necessitate a more complete orifice model that will represent a wide variety of realistic operating conditions. The generalized equation, which includes various nonlinearities, for the supply side flow rate can be expressed as

$$Q_{1S} = \begin{cases} 0 \quad \text{for } x_v \le -\varepsilon_{1S}, \\ \alpha \operatorname{sgn}(P_S - P_1) |P_S - P_1|^{1/2} (x_v + \varepsilon_{1S}) \\ \qquad \text{for } -\varepsilon_{1S} < x_v < L - \varepsilon_{1S}, \\ \alpha \operatorname{sgn}(P_S - P_1) |P_S - P_1|^{1/2} (L) \\ \qquad \text{for } L - \varepsilon_{1S} \le x_v. \end{cases} \tag{2.1a}$$

where $\alpha = C_d w \sqrt{2/\rho}$. Similarly, the return side flow rate is given by

$$Q_{1R} = \begin{cases} 0 \quad \text{for } -x_v \le -\varepsilon_{1R}, \\ \alpha \operatorname{sgn}(P_1 - P_R) |P_1 - P_R|^{1/2} (-x_v + \varepsilon_{1R}) \\ \qquad \text{for } -\varepsilon_{1R} < -x_v < L - \varepsilon_{1R}, \\ \alpha \operatorname{sgn}(P_1 - P_R) |P_1 - P_R|^{1/2} (L) \\ \qquad \text{for } L - \varepsilon_{1R} \le -x_v. \end{cases} \tag{2.1b}$$

Note that while the ranges for the values of the parameter x_v remain similar for both equations in (2.1), the sign of x_v is reversed. This is because the orifice opening on one side of the output port becomes larger while the opening on the other side becomes smaller as

the parameter x_v is varied. Further, the flow equations (2.1) assume turbulent flow through the orifices, no internal leakage, and no cavitation. The total flow rate, Q_1, through the output port is the difference between the supply and return side flow rates, so that

$$Q_1 = Q_{1S} - Q_{1R}. \tag{2.2}$$

These flow-rate equations are quite general and encompass the various nonlinear effects previously mentioned. In particular, the above equations model: valve underlap or overlap, asymmetric neutral land position, and flow reversal. Although the flow-rate equations in (2.1) appear difficult to analyze and interpret, they are simplified if we use a saturation function. The saturation function, shown in Figure 2.2, is defined as follows

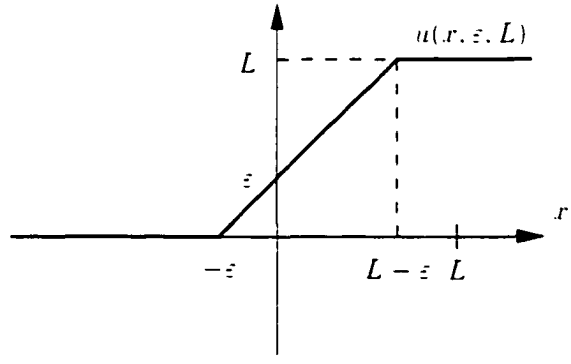

Figure 2.2: Saturation function (shown for $\varepsilon \geq 0$).

$$u(x, \varepsilon, L) = \begin{cases} 0 & \text{for } x \leq -\varepsilon, \\ x + \varepsilon & \text{for } -\varepsilon < x < L - \varepsilon, \\ L & \text{for } L - \varepsilon \leq x. \end{cases} \tag{2.3}$$

Using this function, the orifice equations can be expressed more simply as

$$\begin{aligned} Q_1 &= Q_{1S} - Q_{1R} \\ &= \alpha \Big[\operatorname{sgn}(P_S - P_1) |P_S - P_1|^{1/2} \; u(x_v, \varepsilon_{1S}, L) \\ &\quad - \operatorname{sgn}(P_1 - P_R) |P_1 - P_R|^{1/2} \; u(-x_v, \varepsilon_{1R}, L) \Big] . \end{aligned} \tag{2.4}$$

2.2.1 Proportional Valve Model

Having developed a concise relation for orifice flow, we will now incorporate this relation in the proportional valve shown in Figure 2.3. The model results from combining two orifice

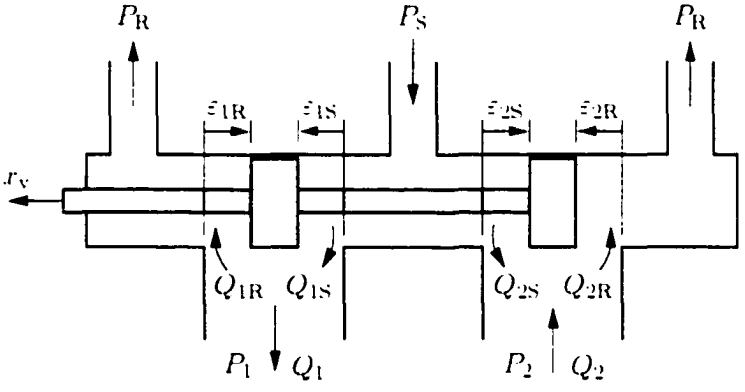

Figure 2.3: Hydraulic proportional valve.

equations so that the lands are rigidly connected and undergo identical displacements. The flow equation for Port 1 is identical to the orifice equation (2.4). The flow equation for Port 2 has a similar form, but the position of the supply and return lines are interchanged, resulting in a modified form in terms of the sign of the spool position variable, x_v:

$$\begin{aligned} Q_2 &= Q_{2R} - Q_{2S} \\ &= \alpha \Big[\operatorname{sgn}(P_2 - P_R) |P_2 - P_R|^{1/2} \; u(x_v, \varepsilon_{2R}, L) \\ &\quad - \operatorname{sgn}(P_S - P_2) |P_S - P_2|^{1/2} \; u(-x_v, \varepsilon_{2S}, L) \Big] . \end{aligned} \tag{2.5}$$

The flow-rate equations (2.4) and (2.5) can be used to simulate *all* important nonlinear

behavior of hydraulic proportional valves. In particular, valve land overlap or underlap and valve land asymmetry can be simulated by varying valve parameters. Port 1 characteristics are changed via the parameters ε_{1S} and ε_{1R}. A symmetric overlapped land has $\varepsilon_{1S} = \varepsilon_{1R} < 0$, and a symmetric underlapped land has $\varepsilon_{1S} = \varepsilon_{1R} > 0$. Asymmetric spool properties and neutral position offset between valve lands can also be modeled using underlap or overlap values so that $\varepsilon_{1S} \neq \varepsilon_{1R}$. Similar considerations apply for the Port 2 parameters ε_{2S} and ε_{2R}.

The overall intent of this chapter is to develop a relationship between valve-spool displacement and fluid flow. The bond graph model of the proportional valve, shown in Figure 2.4, will be used in the sequel to develop this relationship.

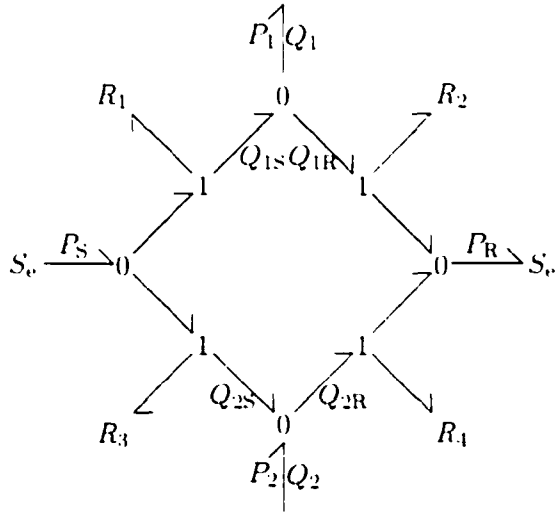

Figure 2.4: Proportional valve bond graph (modified from [11]).

2.3 Hydraulic Cylinder Model

In applications, the hydraulic actuator is typically a double-acting hydraulic cylinder. The cylinder ports are connected to a proportional valve, and piston motion is obtained by modulating the oil flow into and out of the cylinder chambers. A proportional valve provides this modulation.

The motion of the double-acting hydraulic actuator shown in Figure 2.5 can be precisely controlled by regulating the flow rates Q_1 and Q_2. However, the relationship between the

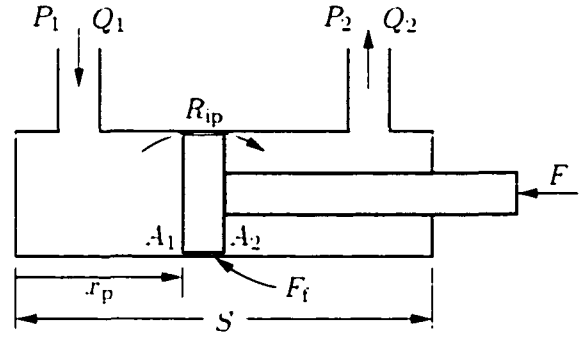

Figure 2.5: Double-acting hydraulic piston.

piston position, x_p, and the flow rates depends on the dynamic properties of the loads acting on the piston. The bond graph in Figure 2.6, which represents the power flow in a hydraulic piston, facilitates analysis of this relationship.

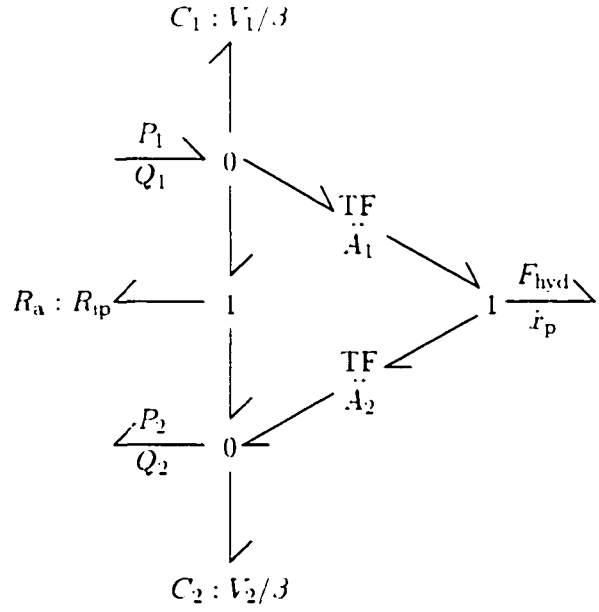

Figure 2.6: Hydraulic piston bond graph (modified from [11]).

The oil and actuator properties determine the exact form of this relationship. Hydraulic

fluid compressibility and leakage flow across the chambers also affect the flow rates. Fluid compressibility is characterized by the equation

$$dV = -\frac{V}{\beta} dP. \tag{2.6}$$

where β is the fluid bulk modulus, V is the chamber volume, and P is the fluid pressure. For hydraulic fluids, the bulk modulus has a nearly constant value. The leakage flow across the cylinder chambers is a linear function of the pressure differential across the piston [8], expressed as

$$Q_{lp} = R_{lp}(P_1 - P_2).$$

where R_{lp} is the coefficient of internal leakage.

The application of the continuity equation to the two sides of the cylinder yields

$$\frac{V_1}{\beta} \dot{P}_1 = -\dot{V}_1 - R_{lp}(P_1 - P_2) + Q_1. \tag{2.7a}$$

$$\frac{V_2}{\beta} \dot{P}_2 = -\dot{V}_2 + R_{lp}(P_1 - P_2) - Q_2. \tag{2.7b}$$

where

$$V_1 = V_{10} + A_1 x_p. \tag{2.8a}$$

$$V_2 = V_{20} + A_2(S - x_p). \tag{2.8b}$$

are the total fluid volumes in the two sides of the cylinder [44]. Here, S is the piston stroke, and V_{10} and V_{20} are the fluid volumes in the lines and fittings on the two sides of the cylinder. The first left-hand terms in (2.7) express the effect of oil compressibility on the flow rates. The first right-hand terms represent the flow rates as a function of volume change due to the piston motion.

The net force, F, provided by the actuator is the difference between the hydraulic force

and the frictional force, that is,

$$\begin{aligned} F &= F_{\text{hyd}} - F_{\text{f}}(\dot{x}_{\text{p}}) \\ &= A_1 P_1 - A_2 P_2 - F_{\text{f}}(\dot{x}_{\text{p}}). \end{aligned} \tag{2.9}$$

The friction force may be modeled as a combination of Coulomb friction, which is approximated by the signum function, and viscous friction:

$$F_{\text{f}}(\dot{x}_{\text{p}}) = \mu \operatorname{sgn} \dot{x}_{\text{p}} + b\dot{x}_{\text{p}},$$

where μ is the Coulomb friction and b is viscous friction coefficient. More general friction models can be incorporated into the friction force term, $F_{\text{f}}(\dot{x}_{\text{p}})$, if necessary.

2.4 Analysis of the Hydraulic System Properties

The dynamics of a hydraulic system comprising a generic proportional valve and a cylinder is described by the model equations (2.4)-(2.5) and (2.7)-(2.9). Although various analyses have been performed using similar models, they are in general limited to systems with critical center valves. Using unified valve equations developed in previous section, however, we are able to extend analyses to all such systems, regardless of the valve type.

The general trend in hydraulic servo control systems is to eliminate underlapped and overlapped spools in proportional valves. Instead, precision manufactured and expensive critical center spools are used together with a matching valve body. However, advances in nonlinear control theory made it possible to use open and closed center valves to our advantage, or at least to cope with the nonlinearities they introduce [41, 47, 49].

In this section, we obtain various flow properties of generic proportional valves in a form suitable for nonlinear control applications. We assume the valve-cylinder configuration has the following characteristics:

1. a double-acting cylinder with equal chamber areas: $A = A_1 = A_2$,

2. an incompressible fluid: $\beta \to \infty$.

3. a matched spool with lapping parameters: $\varepsilon_1 = \varepsilon_{1S} = \varepsilon_{2R}$, and $\varepsilon_2 = \varepsilon_{1R} = \varepsilon_{2S}$.

4. no flow reversal or cavitation: $P_S \geq P_i \geq P_R \geq 0$, $i = 1, 2$.

Using Assumptions 1 and 2, the cylinder bond graph structure of Figure 2.6 reduces to a simpler form as shown in Figure 2.7. This allows simplified flow-rate equation to be

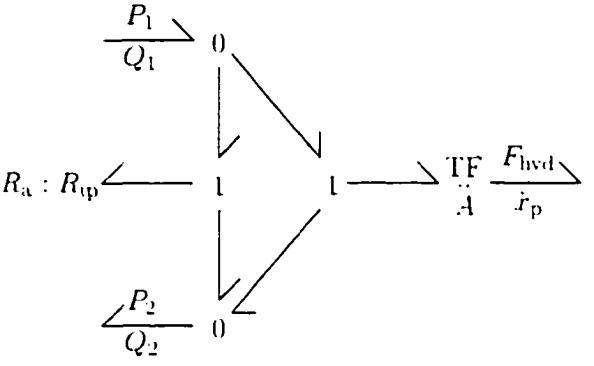

Figure 2.7: Simplified hydraulic piston bond graph.

derived from (2.7):

$$Q_1 = Q_2 = A\dot{x}_p + R_{tp}(P_1 - P_2).$$

where we used (2.8) to obtain the expressions for the derivatives of chamber volumes. This equality allows us to derive simplifying relations for the valve flow rate equations in (2.4) and (2.5). From the proportional valve bond graph of Figure 2.4, we obtain

$$Q_1 = Q_{1S} - Q_{1R}.$$
$$Q_2 = Q_{2R} - Q_{2S}.$$

so that

$$Q_{1S} - Q_{2R} = -(Q_{2S} - Q_{1R}).$$

since we have $Q_1 = Q_2$. Therefore, using (2.4)-(2.5) and Assumptions 3 and 4, this equation can be explicitely written in terms of systems variables as

$$\left(\sqrt{P_S - P_1} - \sqrt{P_2 - P_R}\right) u(x_v, \varepsilon_1, L) = - \left(\sqrt{P_S - P_2} - \sqrt{P_1 - P_R}\right) u(-x_v, \varepsilon_2, L). \quad (2.10)$$

This equation must be satisfied for every combination of system parameters and variables. We have available two possible means to satisfy (2.10):

1. The terms

$$\sqrt{P_S - P_1} - \sqrt{P_2 - P_R} = 0,$$
$$\sqrt{P_S - P_2} - \sqrt{P_1 - P_R} = 0,$$

which results when $P_S + P_R = P_1 + P_2$.

2. The terms

$$u(x_v, \varepsilon_1, L) = u(-x_v, \varepsilon_2, L) = 0, \quad (2.11)$$

which results when $P_S + P_R \neq P_1 + P_2$. To see this, we rearrange (2.10) in the form

$$u(x_v, \varepsilon_1, L) = - \left[\frac{\sqrt{P_S - P_2} - \sqrt{P_1 - P_R}}{\sqrt{P_S - P_1} - \sqrt{P_2 - P_R}}\right] u(-x_v, \varepsilon_2, L).$$

Since the bracketed term is positive for $P_S + P_R \neq P_1 + P_2$ and each $u(\cdot) \geq 0$, it is clear that (2.11) must hold.

Let us now consider these two cases vis-a-vis valve lapping:

(a) For an overlapped or critical-center spool: we have $\varepsilon_1, \varepsilon_2 \leq 0$, so that the equality in (2.11) is satisfied only for $x_v \in (\varepsilon_2, -\varepsilon_1)$. Therefore, outside of this region, $P_S + P_R = P_1 + P_2$ must hold. Furthermore, within the region $x_v \in (\varepsilon_2, -\varepsilon_1)$, all flow rates equal

zero.

(b) For an underlapped spool: we have $\varepsilon_1, \varepsilon_2 > 0$. so that the equality in (2.11) is never satisfied for any value of x_v. Thus $P_S + P_R = P_1 + P_2$ must hold.

The consequences of (a) and (b) are the following: either $P_S + P_R = P_1 + P_2$ or all valve flow rates equal zero. Substituting this pressure equality into the flow rate equations, (2.4) and (2.5), and comparing terms, we obtain

$$Q_{1S} = Q_{2R},$$
$$Q_{1R} = Q_{2S},$$

which also holds for zero flow rates. Furthermore, since $Q_1 = Q_2$, the flow rate equations can be expressed as

$$Q_1 = Q_2 = m_1 u(x_v, \varepsilon_1, L) - m_2 u(-x_v, \varepsilon_2, L). \tag{2.12}$$

where

$$m_1 = \alpha\sqrt{\frac{P_S - P_R - P_L}{2}}, \quad m_2 = \alpha\sqrt{\frac{P_S - P_R + P_L}{2}}$$

are the slopes and $P_L \doteq P_1 - P_2$ is the load pressure.

Equation (2.12) provides a useful relation for flow-rate versus spool displacement. This relation is plotted in Figure 2.8, where an overlapped valve is assumed. We see five distinct regimes. Inside the deadzone, the flow rates are zero. This corresponds to the case $P_S + P_R \neq P_1 + P_2$, where the motion of the spool and the cylinder decouples, so that the equality $P_S + P_R = P_1 + P_2$ can no longer be maintained. Outside the deadzone, the motion of the piston is governed by (2.12), which provides the flow rate input to the cylinder.

For an underlapped valve, the analysis is slightly more complex. Outside the underlap region, $x_v \notin (-\varepsilon_1, \varepsilon_2)$, the sloped regions of Figure 2.8, m_1 and m_2, as well as the saturations are all present as shown in Figure 2.9. However, within the underlap region, we have

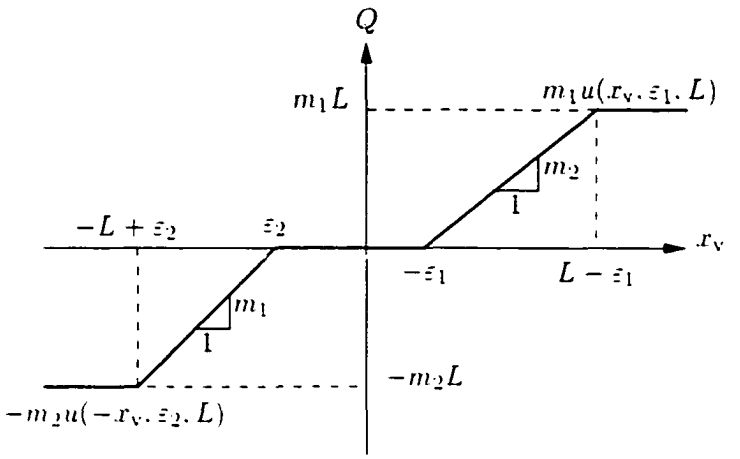

Figure 2.8: Plot of Eq. (2.12) for an overlapped valve.

$$u(x_v, \varepsilon_1, L) = x_v + \varepsilon_1,$$

$$u(-x_v, \varepsilon_2, L) = -x_v + \varepsilon_2,$$

so that

$$\begin{aligned} Q_1 = Q_2 &= m_1(x_v + \varepsilon_1) - m_2(-x_v + \varepsilon_2) \\ &= (m_1 + m_2)x_v + (m_1\varepsilon_1 - m_2\varepsilon_2), \end{aligned}$$

where the term $(m_1\varepsilon_1 - m_2\varepsilon_2)$ is the null flow rate due to the load pressure, P_L. This means that even for a centered spool, $x_v = 0$, we may have piston motion due to the null flow if $\varepsilon_1 \neq \varepsilon_2$ and $P_L \neq 0$.

On the other hand, the term $(m_1 + m_2)x_v$ represents the flow gain relation between spool position and flow rate. The flow gain, K_q, within the underlap region is an important number in designing hydraulic control systems, since it determines the open-loop plant gain. Large variations in the flow gain could lead to instability. Fortunately, its bounds can easily

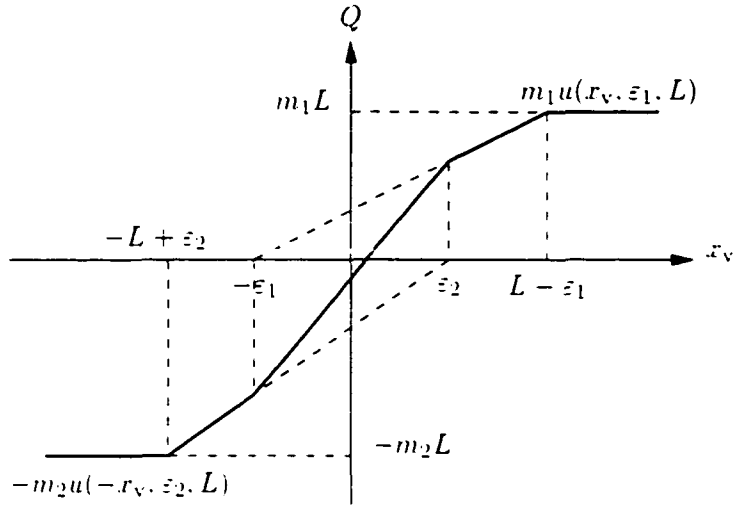

Figure 2.9: Plot of Eq. (2.12) for an underlapped valve.

be characterized as a corollary of our analysis. The flow gain is defined as

$$K_q \doteq \frac{\partial Q}{\partial x_v} = (m_1 + m_2)$$
$$= \frac{\alpha}{\sqrt{2}} \left[\sqrt{P_S - P_R - P_L} + \sqrt{P_S - P_R + P_L} \right].$$

Since $|P_L| \leq P_S - P_R$ by our assumptions, it is easy to show that

$$\alpha \sqrt{P_S - P_R} \leq K_q \leq \sqrt{2} \alpha \sqrt{P_S - P_R}.$$

2.5 Conclusions

We have developed a unified model for proportional control valves and analyzed the effect of spool lapping on open-loop hydraulic system properties. The nonlinear mathematical equations relate the flow rates through the valve ports to the valve parameters. The flow rates are expressed as a continuous but nonlinear function of *lapping parameters*, as well as other conventional parameters. These equations are readily applicable to various types of proportional valves, and they unify the cases of critical center, overlapped, and underlapped

valves.

The spool lands' geometry are individually controlled via model parameters. An offset between the lands, and asymmetric neutral spool position can also be simulated using our model. The system model is fully implemented in Matlab's Simulink simulation package and the hydraulic system component models are combined in a library for easy reuse.

We also derived simplified flow rate equations under certain widely-used assumptions while keeping nonlinearities due to spool geometry. The variation of the flow gain and uncertainty bounds of the flow rates of an underlapped valve are also analyzed.

Although we assumed a constant bulk modulus, changes in temperature, pressure, and percent air in the fluid will alter this parameter. The assumption facilitated the analysis, in particular the piecewise-linear characterization of flow versus spool displacement in Figures 2.8 and 2.9. If operating conditions are such that this assumption is invalid, adaptive [40] and singular perturbation [22] control approaches are available to accommodate the variation in bulk modulus.

Our future work includes developing internal leakage flow models for proportional valves to provide improved servo performance. The design of nonlinear controllers for overlapped and underlapped valve spool is also a promising research area. Simple nonlinear compensators together with less expensive proportional valves offers substantial cost savings in hydraulic control systems design.

Chapter 3

A Unified Model of a Proportional Valve: Analysis of Accuracy

3.1 Introduction

Although the dynamics of proportional valves are highly nonlinear, simplified expressions are employed in practice to express the flow rates through the valve ports. For a critical center valve connected to a double-acting cylinder, the often used load flow equation [38]

$$Q_L = K_q x_v - K_c P_L \tag{3.1}$$

provides a linearized approximation of the valve dynamics as a function of spool opening and load pressure. In this expression, the load flow and load pressure are defined respectively as

$$Q_L \doteq (Q_1 + Q_2)/2, \quad P_L \doteq P_1 - P_2,$$

where the subscripts refer to the valve output ports. However, the load flow in Eq. (3.1) represents the average of the flows in the lines and does not equal to the instantaneous flow rate at each valve ports. Furthermore, this flow equation is only valid for a critical center

valve.

An improved flow model is developed in [23], where the effect of valve lapping on the flow rates is incorporated into the model. This model provides a single set of flow rate equations for a generic proportional valve, combining the cases of critical center, overlapped, and underlapped proportional valves. Under generally accepted assumptions such as incompressible fluid, the model simplifies considerably, which results in a piecewise-linear approximation of the flow rates at the valve ports.

In applications, one of the major concerns for the engineer is the difficulty of determining the accuracy of these simplified flow models. Whenever cost and packing size constraints are stringent, the tendency is to use cheaper proportional valves and smaller actuators. Less expensive valves introduce a higher degree of uncertainty regarding the valve lapping, and smaller actuators limit the bandwidth of the hydraulic system. Both of these choices may result in a system where the simplified flow relations no longer provide an accurate representation of the valve dynamics. Therefore, given a set of desired system parameters, it is important for the engineer to be able to determine, a priori, the accuracy of the flow model that will be used subsequently for analysis and control design.

In this chapter, we analyze the accuracy of the piecewise-linear flow model developed in [23]. The accuracy of the model is determined through a non-dimensional analysis, and thus the results hold for any similar system. Given a set of hydraulic system parameters, the analysis allows a designer to determine if this flow model will provide an accurate representation of the valve dynamics for subsequent analysis and control design.

3.2 Unified Proportional Valve Model

The proportional valve model developed in [23] provides a single set of flow relations for a generic proportional valve shown in Figure 3.1. In terms of the model parameters, the flow

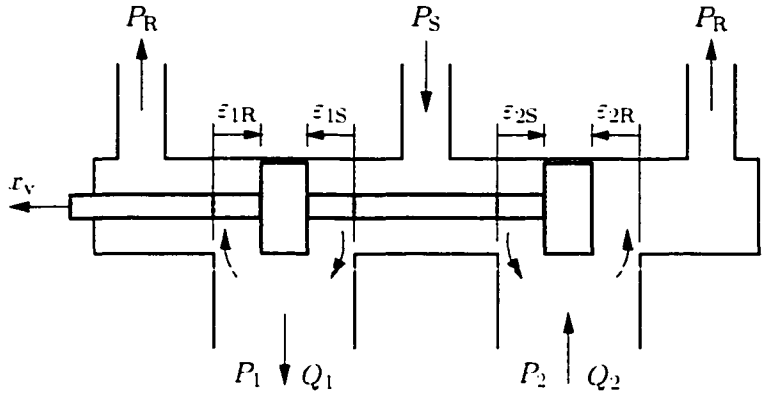

Figure 3.1: Hydraulic proportional valve.

rates at the valve output ports are expressed as

$$\begin{aligned} Q_1 = \alpha \Big[& \operatorname{sgn}(P_S - P_1) |P_S - P_1|^{1/2} \, u(x_v, \varepsilon_{1S}, L) \\ & - \operatorname{sgn}(P_1 - P_R) |P_1 - P_R|^{1/2} \, u(-x_v, \varepsilon_{1R}, L) \Big] . \end{aligned} \tag{3.2a}$$

$$\begin{aligned} Q_2 = \alpha \Big[& \operatorname{sgn}(P_2 - P_R) |P_2 - P_R|^{1/2} \, u(x_v, \varepsilon_{2R}, L) \\ & - \operatorname{sgn}(P_S - P_2) |P_S - P_2|^{1/2} \, u(-x_v, \varepsilon_{2S}, L) \Big] . \end{aligned} \tag{3.2b}$$

where $\alpha = C_d w \sqrt{2/\rho}$ and C_d is the discharge coefficient, w is the valve area gradient, and ρ is the fluid density. The saturation function $u(x, \varepsilon, L)$ is defined as follows

$$u(x, \varepsilon, L) = \begin{cases} 0 & \text{for } x \leq -\varepsilon, \\ x + \varepsilon & \text{for } -\varepsilon < x < L - \varepsilon, \\ L & \text{for } L - \varepsilon \leq x. \end{cases}$$

In this model, the ε-parameters represent the spool underlap or overlap (at neutral spool position) on the supply and return sides of the valve ports. With respect to the neutral spool position, *positive* values of these parameters correspond to spool *underlap* (shown

in Figure 3.1). Similarly, *negative* parameter values define an *overlapped* spool.

The model (3.2) unifies the cases of critical center, overlapped, and underlapped valves. The resulting nonlinear equations relate the flow rates through the valve ports to the valve parameters. These flow rates are expressed as a continuous but nonlinear function of *lapping parameters*, as well as other conventional parameters.

In [23], the flow relations (3.2) are also further simplified under certain widely-used assumptions while keeping nonlinearities due to spool geometry. The assumption of incompressible fluid, among others, results in simplified flow rate equations, where the flow rates are piecewise-linear functions of spool position. The resulting flow rate equations are expressed as

$$Q_1 = Q_2 = m_1 u(x_v, \varepsilon, L) - m_2 u(-x_v, \varepsilon, L). \tag{3.3}$$

where

$$m_1 = \alpha\sqrt{\frac{P_S - P_R - P_L}{2}}, \quad m_2 = \alpha\sqrt{\frac{P_S - P_R + P_L}{2}}$$

are the flow gains.

The accuracy of the flow model (3.3) depends on its ability to estimate the flow rates observed in a fully nonlinear model of a given hydraulic system. Hence a comparison of flow rates obtained from a detailed nonlinear model of a generic hydraulic system with the flow rates predicted by the piecewise-linear flow model (3.3) is necessary.

As a representative application, we select the system configuration shown in Figure 3.2, where a large load is driven by the hydraulic actuator. However, to be useful in practice, an accuracy analysis of the model in Eq. (3.3) should not depend on the properties of a given system. That is, the comparison of the dynamics of a detailed nonlinear model of the system in Figure 3.2 and the unified proportional valve model should give universal results in terms of predicting the accuracy of the latter model. This requires a non-dimensional type of analysis, which does not depend on the system parameters.

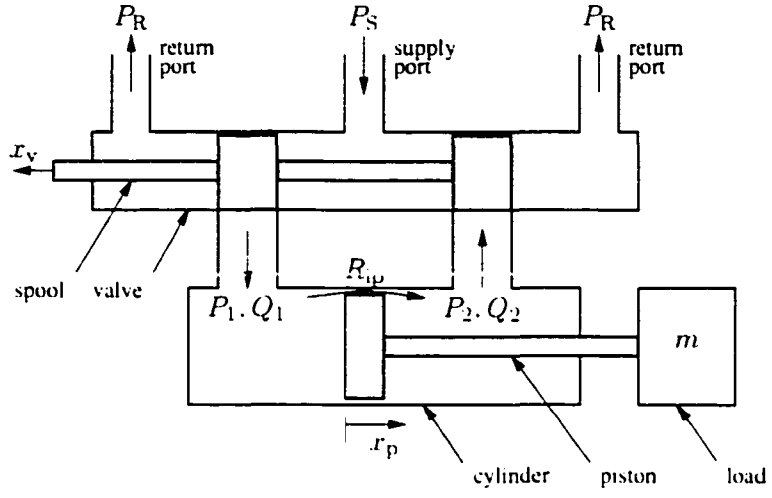

Figure 3.2: A representative hydraulic system

In order to clarify what is meant by a non-dimensional analysis, we first turn to a linear model of the hydraulic system in Figure 3.2 and analyze its invariance properties with respect to model parameters.

3.3 Non-Dimensional Analysis: Insights from a Linear Model

Considering the hydraulic system of Figure 3.2, an application of the continuity equation to the two sides of the cylinder yields

$$\dot{P}_1 = \frac{\beta}{V_1}\left[-\dot{V}_1 - R_{ip}(P_1 - P_2) + Q_1\right], \tag{3.4a}$$

$$\dot{P}_2 = \frac{\beta}{V_2}\left[-\dot{V}_2 + R_{ip}(P_1 - P_2) - Q_2\right]. \tag{3.4b}$$

where R_{ip} is the internal leakage coefficient between the cylinder chambers [23]. Other parameters are defined in the nomenclature.

We assume that the piston is initially centered so that the chamber volumes can be

modeled as

$$V_1 = V_{10} + A_1 x_p.$$
$$V_2 = V_{20} - A_2 x_p.$$

where the initial chamber volumes are $V_{10} = V_{20} = V_t/2$, and V_t is the total cylinder volume including the connections, fittings, etc. For a double-acting cylinder with equal piston areas, we have $A_p \equiv A_1 = A_2$, so that $\dot{V}_1 = A_p \dot{x}_p$ and $\dot{V}_2 = -A_p \dot{x}_p$.

Assuming that the motion of the piston is limited to the region around the center of the cylinder, we may write

$$V_1 \approx V_2 \approx \frac{V_t}{2}. \tag{3.5}$$

Hence the pressure relations (3.4) can be rewritten as

$$\dot{P}_1 = \frac{2\beta}{V_t}\left[-A_p \dot{x}_p - R_{tp}(P_1 - P_2) + Q_1\right]. \tag{3.6a}$$
$$\dot{P}_2 = \frac{2\beta}{V_t}\left[+A_p \dot{x}_p + R_{tp}(P_1 - P_2) - Q_2\right]. \tag{3.6b}$$

The equation of motion of the load mass is $m\ddot{x}_p = F_{hyd}$, where m is the total mass of the piston and the load, and $F_{hyd} = A_p P_L$ is the hydraulic force due to pressure differential across the piston. Differentiating this and using Eq. (3.6), we obtain

$$\begin{aligned} m\dddot{x}_p = \dot{F}_{hyd} &= A_p \dot{P}_L \\ &= \frac{2\beta A_p}{V_t}\left[-2A_p \dot{x}_p - 2R_{tp} P_L + 2Q_L\right]. \end{aligned} \tag{3.7}$$

Using the relation $P_L = m\ddot{x}_p/A_p$, we can simplify Eq. (3.7) as

$$m\dddot{x}_p + \frac{4\beta R_{tp} m}{V_t}\ddot{x}_p + \frac{4\beta A_p^2}{V_t}\dot{x}_p = \frac{4\beta A_p}{V_t} Q_L. \tag{3.8}$$

Considering the above equation, we see that the dynamics of the hydraulic system is similar

to that of a second order linear system in the variable $\dot{x}_p = v_p$, the piston velocity. However, it should be noted that the load flow, Q_L, is in general a nonlinear function of spool position and chamber pressures, and therefore the above differential equation is in fact nonlinear.

It is possible to treat a simpler case, where the load flow is given by Eq. (3.1). In this case, the response of the system is linear and can be expressed in terms of the piston velocity as

$$\ddot{v}_p + 2\zeta_h\omega_h\dot{v}_p + \omega_h^2 v_p = \omega_h^2 \frac{K_q}{A_p} x_v. \tag{3.9}$$

where the hydraulic natural frequency and the hydraulic damping coefficient are defined respectively as

$$\omega_h = 2A_p\sqrt{\frac{\beta}{mV_t}}, \quad \zeta_h = \frac{(B_{ip} + K_c)}{A_p}\sqrt{\frac{\beta m}{V_t}}.$$

The terms on the right hand side of Eq. (3.9) can be combined as $\bar{v}_p = (K_q/A_p)x_v$, so that we obtain

$$\begin{aligned}\frac{\bar{V}_p(s)}{\bar{V}_p(s)} &= \frac{\omega_h^2}{s^2 + 2\zeta_h\omega_h s + \omega_h^2} \\ &= \frac{1}{(s/\omega_h)^2 + 2\zeta_h(s/\omega_h) + 1}.\end{aligned} \tag{3.10}$$

in terms of the Laplace variable, s. Note that the variable $\bar{v}_p$ is equivalent to the velocity of the piston as a function of spool opening if the hydraulic fluid is incompressible. It also represent the average behavior of the piston velocity.

To obtain a non-dimensional representation of hydraulic system behavior, we define a new complex variable $p \doteq s/\omega_h$ so that Eq. (3.10) becomes

$$\frac{\bar{V}_p(p)}{\bar{V}_p(p)} = \frac{1}{p^2 + 2\zeta_h p + 1}. \tag{3.11}$$

This transfer function suggests that for all systems with a given hydraulic damping coefficient, ζ_h, the relation between the actual and approximate piston velocities is invariant

with system properties. That is, for a given damping coefficient, the frequency response of Eq. (3.11) for $s = j\omega$ (i.e., sine input) is fixed, independent of the value of individual parameters making up the damping coefficient. Hence, Eq. (3.11) provides a non-dimensional linear model of the hydraulic system in Figure 3.2.

If the unified valve model Eq. (3.3) exhibits similar invariance properties for a given value of the damping coefficient, the accuracy of the model will be independent of how the system parameters are selected to give that damping coefficient. These invariance properties are investigated in the next section.

3.4 Analysis of Unified Model Accuracy

To show that the accuracy of the unified model Eq. (3.3) can be analyzed universally, independent of the value of hydraulic system parameters, we have performed various simulations. In these simulations, the response of the hydraulic system in Figure 3.2 has been evaluated using *(1)* a fully nonlinear, detailed model of the proportional valve, and *(2)* the simplified model of Eq. (3.3).

The input was a sinusoidal spool position command of the form

$$x_v = A_v \sin(2\pi f t),$$

where we selected $A_v > L$ to cover the whole range of spool travel, and a number of input frequencies within the range $\omega = 2\pi f \in (0, \omega_h]$.

The nominal model parameters used in simulations are

$L = 10 \times 10^{-3}$ m	$\varepsilon = \pm 0.1 \times L$	$\alpha = 10 \times 10^{-6}$ m$^{5/2}$/kg$^{1/2}$
$P_S = 1.6 \times 10^7$ N/m^2	$P_R = 3.7 \times 10^5$ N/m^2	$\beta = 6.1 \times 10^8$ N/m^2
$A_p = 5.8 \times 10^{-4}$ m^2	$V_t = 40 \times 10^{-6}$ m^3	$R_{lp} = 1.8 \times 10^{-11}$ m^3/sPa
$m = 20$ kg	$S = 50 \times 10^{-3}$ m	$K_c = 1.9 \times 10^{-12}$ m^3/sPa.

However, in parallel with the discussion regarding the linear non-dimensional model (3.11), the system parameters were varied so as to keep the damping coefficient, ζ_h, constant.

The parameter variations used in simulations for both underlapped and overlapped valves are shown in Table 3.1. Note that, whereas the damping coefficient is constant,

Set	Parameter Changes	ζ_h	ω_h, Hz
1	nominal values	0.6	160
2	$m \rightarrow m/10$ and $\beta \rightarrow 10\beta$	0.6	1600
3	$m \rightarrow m/10$ and $A \rightarrow A/\sqrt{10}$	0.6	160
4	$m \rightarrow 10m$ and $\beta \rightarrow \beta/10$	0.6	16
5	$m \rightarrow 10m$ and $V_t \rightarrow 10V_t$	0.6	16

Table 3.1: Simulation parameter sets

the natural frequency of the hydraulic system varies by a factor of 100. Nevertheless, as indicated by the non-dimensional linear model of the system, we expect that simulations using the simplified model would result in a fixed response, regardless of model parameters.

In addition, we have determined the accuracy of the simplified model (3.3) by comparing the simulation results with that of a fully non-linear model of the same proportional valve. We define the errors in the simplified model as

$$e_p = \left[\frac{\int |Q_{L_{non}} - Q_{L_{sim}}|^p \, dt}{\int |Q_{L_{sim}}|^p \, dt} \right]^{1/p}.$$

where $p = 2$ for rms errors and $p = \infty$ for maximum errors. The variable $Q_{L_{non}}$ denotes the load flow rate obtained using the detailed nonlinear model of the valve, and $Q_{L_{sim}}$ denotes the load flow obtained using the unified proportional valve model (3.3).

A typical response of an underlapped valve for nominal system parameters is shown in Figure 3.3. Note that for a full cycle of spool travel, the errors are larger for an accelerating load.

The maximum and rms errors for an underlapped valve for the set of all parameter variations described in Table 3.1 are shown in Figure 3.4. Note that regardless of system

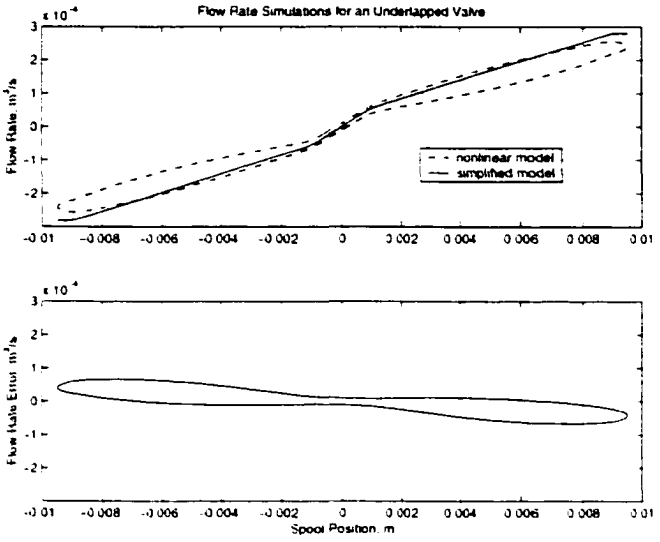

Figure 3.3: Typical response for an underlapped valve at $f = 75$ Hz (nominal system).

parameters, the errors consistently follow an identical path. This indicates that the simplified valve model, indeed, confirms the non-dimensional analysis argument developed using a second order linear model of the same hydraulic system.

Similarly, a typical response of an underlapped valve for nominal system parameters is shown in Figure 3.5. The maximum and rms errors for an overlapped valve for the set of all parameter variations described in Table 3.1 are shown in Figure 3.6. As in the case of an underlapped valve, the errors follow an identical path regardless of model parameter variations.

Note that in Figures 3.4 and 3.6, the maximum errors when using the unified valve model are less than 10 percent for frequencies up to one third of the natural frequency of the hydraulic system. Since most hydraulic systems are rarely driven with input signal frequencies more than half of the natural frequency of the system, the unified valve model provides an accurate representation of the valve dynamics for most applications.

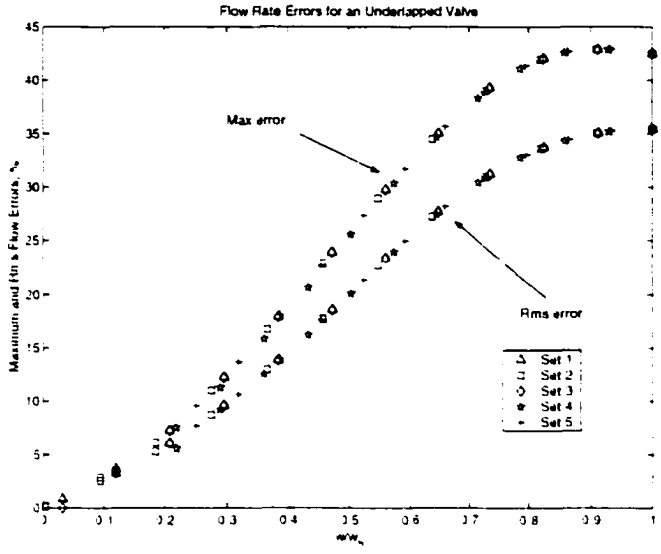

Figure 3.4: Maximum and rms errors for an underlapped valve.

3.5 Conclusions

In this chapter, we have analyzed the accuracy of the unified proportional valve model developed in [23]. As suggested by a second-order linear model of a generic hydraulic system configuration, a non-dimensional analysis of the unified model confirms that the accuracy of the model is independent of the choice of a particular set of model parameters. In fact, for a given value of the hydraulic damping coefficient, the simulations of the model error do not depend on the model parameter values, as long as their combination results in a fixed damping coefficient. Therefore, the accuracy of the model can be determined a priori using similar simulations as described in the chapter. This would provide great flexibility to an engineer in deciding whether the unified model can be used for subsequent analysis and control design without introducing modeling errors due to the presence of valve dynamics.

It is also shown that the errors in using the unified valve model are less than 10 percent for frequencies up to one third of the natural frequency of the system. Since most hydraulic systems are rarely driven above this frequency range, it can be concluded that the unified valve model provides an accurate representation of the valve dynamics for most applications.

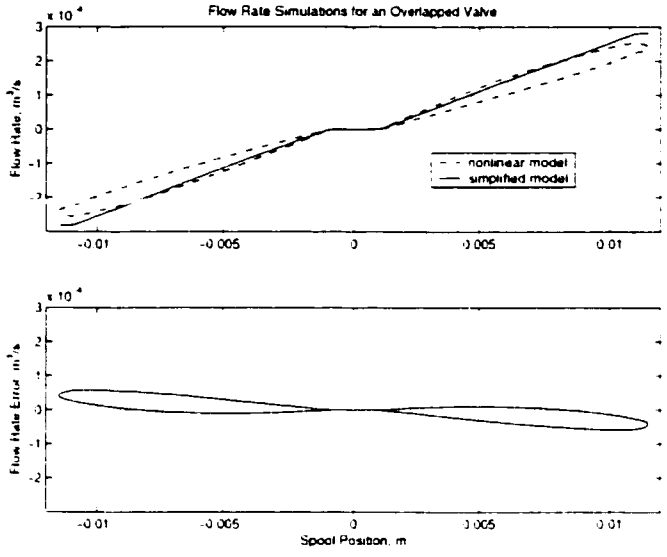

Figure 3.5: Typical response for an overlapped valve at $f = 75$ Hz (nominal system).

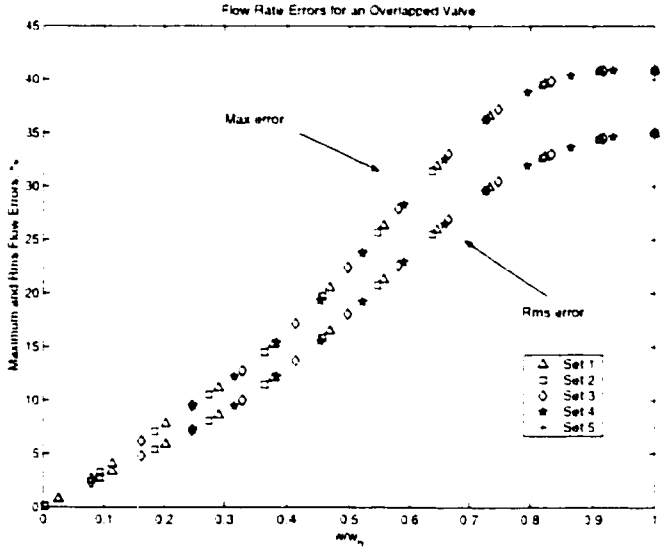

Figure 3.6: Maximum and rms errors for an overlapped valve.

Chapter 4

Combining Leakage and Orifice Flows in a Hydraulic Servovalve Model

4.1 Introduction

In this chapter, we consider flow, in particular, leakage flow, between a servovalve spool and valve body. Such flow is a key consideration in precision positioning applications. An *ideal* servovalve has perfect geometry, so that leakage flows are zero. In this case the theoretical orifice equation

$$Q = K\sqrt{\Delta P}\, x, \tag{4.1}$$

where ΔP is the pressure drop across the orifice, x is the orifice opening, and K is the servovalve gain, holds over the whole range of spool travel. Note that subsequent symbols are defined in nomenclature. However, for *actual* servovalves, this relation only holds outside the null region. In practice, servovalves have considerable leakage flow at small valve openings. Indeed, experimentation and analysis indicate that at small spool displacements this flow

is much larger than orifice flow. Precision positioning applications involve extremely small actuator displacement commands that result in very small valve openings, where leakage dominates. Most servohydraulic designs are based on the ideal orifice relation (e.g. [6, 39, 45]), applied through the entire range of spool motion. The use of such models for design appears somewhat questionable, given the applicability of ideal relations only outside of the null region and the dominance of leakage flow within the null region. An accurate model that *(1)* includes both leakage flow and orifice flow and *(2)* makes a smooth transition between them would likely improve precision servohydraulic system design and performance.

An accurate yet simple model of the leakage flow in a servovalve facilitates both analysis and design of hydraulic control systems. Hydraulic system performance can be more realistically assessed using such a model for simulations and analyses. Furthermore, a nonlinear controller based on the servovalve internal leakage model may greatly improve the hydraulic system performance, especially in applications that require precise actuator positioning. Various nonlinear controllers are available based on the ideal orifice flow model [6, 45, 56, 57], which provide higher performance than conventional PID compensators. With the availability of an internal leakage model, these controllers may be redesigned to accommodate additional nonlinearities due to servovalve leakage.

Although models of leakage flow in servovalves are available in the literature, these models impose limitations on the spool geometry and valve properties. The leakage flow model developed in [20] assumes a small and symmetric overlap between the spool lands and the valve control ports. However, this model is only valid for a small positive spool displacement limited to approximately 2 percent of maximum spool travel. Furthermore, the model predicts non-smooth flow rate curves for small orifice openings, due to the non-smooth transition from the assumed laminar leakage to turbulent orifice flow.

The model developed in [18] circumvents this problem and provides smooth transition from leakage to orifice flow. But the resulting model is too complex to be used for practical design of nonlinear controllers to improve hydraulic system performance. This model approximates the leakage flow path in a servovalve as a short annulus of fine clearance and

employs the laminar flow model

$$Q = \frac{k_2}{2}\left[\sqrt{\left(\frac{k_2}{k_1}\right)^2 x^2 + 4\Delta P} - \frac{k_2}{k_1}x\right].$$

where the parameters k_1 and k_2 are functions of various geometric and fluid properties [19]. Since these parameters appear nonlinearly in the flow relation, their identification is very difficult and will likely require data that is not readily available from the manufacturers.

In this chapter, we develop a simple nonlinear servovalve model that accurately captures the servovalve leakage behavior. The leakage behavior is modeled as turbulent flow with a flow area inversely proportional to the overlap between the spool land and the servovalve orifices. The model only assumes a critical center spool, and is valid over the entire range of spool travel. In particular, at zero spool displacement, the expressions for turbulent orifice flow for positive openings and leakage flow due to spool-valve overlap predict identical flows, producing a continuous flow relation. Moreover, the model parameters can be calculated from the manufacturer's data for servovalves with symmetrical and matched construction.

The remainder of the chapter is organized as follows. In Section 4.2 we develop a nonlinear model of a hydraulic servovalve with internal leakage. In Section 4.3 we derive the internal leakage and pressure sensitivity relations using the model developed. A method to calculate the servovalve model parameters from manufacturer data is presented in Section 4.4. We compare the response of the model with experimental data in Section 4.5. Conclusions and directions for future research are discussed in Section 4.6.

4.2 Servovalve Model with Internal Leakage

A servovalve spool and a hydraulic actuator, shown in Figure 4.1, are key components of a typical hydraulic control system. The servovalve acts as a power amplifier that converts a low-power electrical signal to spool displacement, which results in flow through the servovalve control ports. The flow into the actuator chambers controls the motion of a hydraulic piston. The control flow rates are nonlinear functions of spool displacement and control

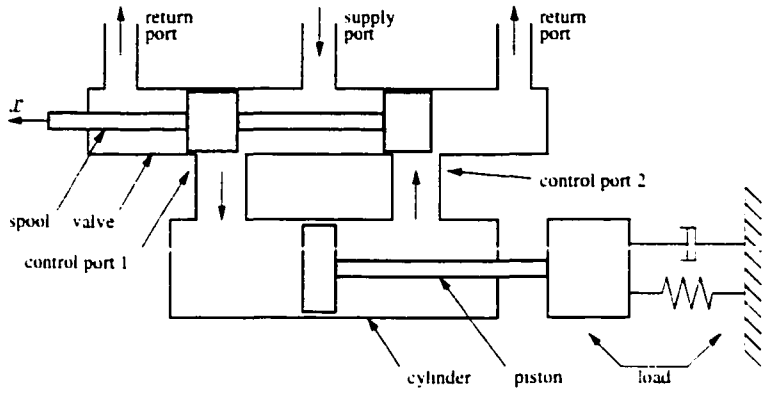

Figure 4.1: Hydraulic system configuration of a material testing machine.

port pressures. The derivation of the governing equations for a servovalve without internal leakage is described in standard texts such as [38]. The derivation results in the square-root type of pressure-flow relation shown in Eq. (4.1). However, within the null region, the leakage flow between the spool and the valve body dominates the servovalve behavior. That is, in this region, the standard *square-root law* (4.1) used to express orifice flow does not provide a valid representation of the flow rates. An improved mathematical model that accurately characterizes the servovalve behavior over the whole range of spool motion (especially around null) would improve hydraulic system analyses and facilitate subsequent control design. Such a model is developed in this section.

A common servovalve spool configuration, shown in Figure 4.2, consists of two control ports with variable orifices that regulate the flow rates. The flow rates through the control ports of the servovalve are expressed in terms of the supply-side and return-side flow rates as

$$Q_1 = Q_{1S} - Q_{1R}. \tag{4.2a}$$

$$Q_2 = Q_{2R} - Q_{2S}. \tag{4.2b}$$

where the flow components are shown in Figure 4.2. The total flow rates through the supply

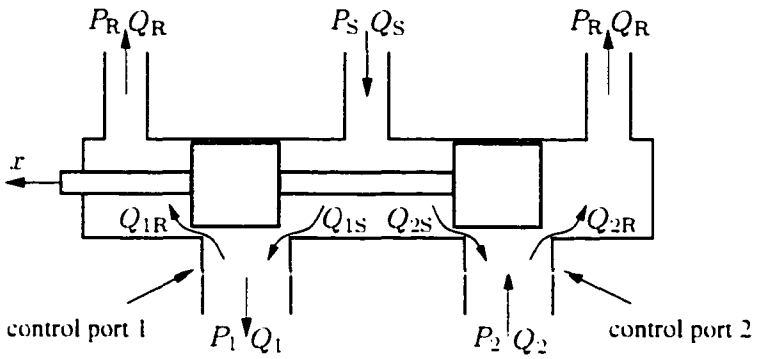

Figure 4.2: Hydraulic servovalve configuration.

and return ports are expressed as

$$Q_S = Q_{1S} + Q_{2S}. \tag{4.3a}$$

$$Q_R = Q_{1R} + Q_{2R}. \tag{4.3b}$$

Combining the flow relations (4.2) and (4.3), we obtain the supply port flow rate in terms of the flows at the control and return ports:

$$Q_S = Q_R + (Q_1 - Q_2).$$

The net flow rate at each control port involves two distinct flow regimes: orifice and leakage flows. Consider, for example, the flows associated with the control port 1 of a servovalve for a positive spool displacement, as shown in Figure 4.2. The flow rate at the supply orifice of this port is given by the orifice equation

$$Q_{1S} = K_{1S}(P_S - P_1)^{1/2}(x_0 + x) \quad (x \geq 0).$$

where the parameter x_0 accounts for the leakage flow rate at null ($x = 0$). Note that x_0 is equivalent to a spool displacement that would result in the same amount of flow in a *non-leaking* servovalve as the leakage flow rate in a *leaking* servovalve with a centered spool. The flow rate at the return orifice of the control port 1 *cannot* be expressed using a simple

orifice flow equation. Larger positive spool displacements increase the length of the leakage flow path to the left of the control port 1, hence increasing the resistance to flow. The leakage path is the result of the overlap between the valve body and the spool land, which forms a short annulus of fine clearance [19].

As Merritt indicates [38], the flow through the annulus is only laminar for a new valve and quickly becomes turbulent during service because abrasive materials in the fluid erode the orifice edges, increasing their areas. In addition, since the length of the overlap is, in general, very short under most operating conditions, the turbulent leakage flow assumption appears valid.

Since leakage resistance increases at larger valve openings, the leakage flow rate is inversely proportional to spool displacement. The flow rate at the return side of the control port 1 can thus be expressed as

$$Q_{1R} = K_{1R}(P_1 - P_R)^{1/2} x_0^2 (x_0 + k_{1R} x)^{-1} \quad (x \geq 0).$$

The term x_0 is again added to account for the presence of turbulent leakage flow at zero spool displacement. The value of the parameter k_{1R} determines the flow resistance of the leakage path in the overlap region as a function of spool displacement.

The above relations for orifice and leakage flow at the servovalve ports form the basis of the servovalve flow model. For negative spool displacements, the flow relations are interchanged since now the supply side forms the leakage path and the return side flow is a turbulent orifice flow. Applying similar reasoning to each orifice, we obtain the following flow relations for control port 1:

$$Q_{1S} = K_{1S}(P_S - P_1)^{1/2} \begin{cases} (x_0 + x), & (x \geq 0), \\ x_0^2 (x_0 - k_{1S} x)^{-1}, & (x < 0). \end{cases} \tag{4.4a}$$

$$Q_{1R} = K_{1R}(P_1 - P_R)^{1/2} \begin{cases} x_0^2 (x_0 + k_{1R} x)^{-1}, & (x \geq 0), \\ (x_0 - x), & (x < 0). \end{cases} \tag{4.4b}$$

For control port 2, we have

$$Q_{2S} = K_{2S}(P_S - P_2)^{1/2} \begin{cases} x_0^2(x_0 + k_{2S}x)^{-1}, & (x \geq 0), \\ (x_0 - x), & (x < 0). \end{cases} \tag{4.5a}$$

$$Q_{2R} = K_{2R}(P_2 - P_R)^{1/2} \begin{cases} (x_0 + x), & (x \geq 0), \\ x_0^2(x_0 - k_{2R}x)^{-1}, & (x < 0). \end{cases} \tag{4.5b}$$

Note that these flow equations are continuous at the neutral spool position. For example, we have

$$\lim_{x \to 0^+} Q_{1S}(x) = \lim_{x \to 0^-} Q_{1S}(x) = K_{1S}(P_S - P_1)^{1/2}x_0.$$

4.3 Internal Leakage and Pressure Sensitivity Models

The validity of the servovalve model developed in Section 4.2 can be determined by comparing measured and predicted flow characteristics of a servovalve. Among various characterizations, the *pressure sensitivity* and the *internal leakage* tests provide the most relevant data to evaluate the servovalve model validity. These tests are among the standard tests performed on servovalves by the manufacturers and their data is available with the servovalves.

The pressure sensitivity test measures the variation of load pressure ($P_L \doteq P_1 - P_2$), with the control ports blocked ($Q_1 = Q_2 = 0$), as the spool travels a complete cycle around null [50]. Due to internal leakage, a typical pressure sensitivity curve shown in Figure 4.3 has a steep but smooth transition between saturations.

The internal leakage test measures the total internal valve flow (Q_S) from supply to return port with the control ports blocked and spool position cycled over its full range [50]. A typical leakage flow curve shown in Figure 4.4 has a maximum at neutral spool position and decreases rapidly with valve stroke.

We now develop mathematical expressions that provide pressure sensitivity and internal

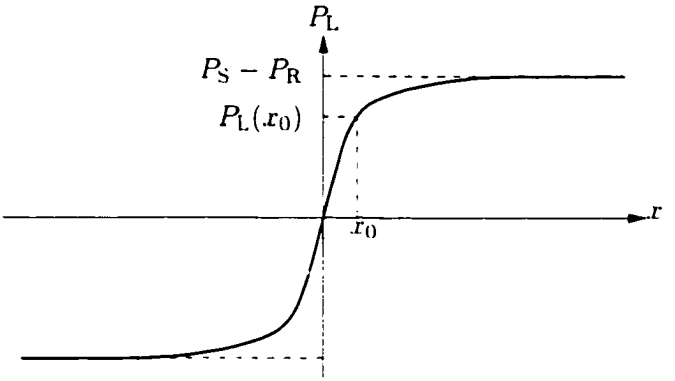

Figure 4.3: Typical pressure sensitivity curve.

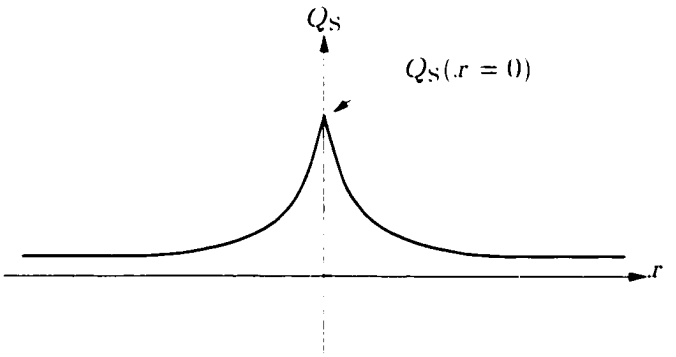

Figure 4.4: Typical leakage flow curve.

leakage relations for a practical servovalve. Since both tests are performed with the control ports blocked (i.e. $Q_1 = Q_2 = 0$). Eq. (4.2a) yields $Q_{1S} = Q_{1R}$ for the control port 1. Substituting this into flow equations in (4.4) and solving for P_1 we obtain

$$P_1 = \begin{cases} \dfrac{f_{1p}P_S + P_R}{1 + f_{1p}}. & (x \geq 0). \\ \dfrac{P_S + f_{1n}P_R}{1 + f_{1n}}. & (x < 0). \end{cases} \tag{4.6}$$

where

$$f_{1p}(x) = \left(\frac{K_{1S}}{K_{1R}}\right)^2 \left[\left(1 + \frac{x}{x_0}\right)\left(1 + k_{1R}\frac{x}{x_0}\right)\right]^2. \tag{4.7a}$$

$$f_{1n}(x) = \left(\frac{K_{1R}}{K_{1S}}\right)^2 \left[\left(1 - \frac{x}{x_0}\right)\left(1 - k_{1S}\frac{x}{x_0}\right)\right]^2. \tag{4.7b}$$

Here the subscripts p and n denote positive and negative values of spool position, x, respectively.

Similarly, Eq. (4.2b) yields $Q_{2S} = Q_{2R}$ for the control port 2. Substituting this into flow equations in (4.5) and solving for P_2 we obtain

$$P_2 = \begin{cases} \dfrac{P_S + f_{2p}P_R}{1 + f_{2p}}, & (x \geq 0), \\ \dfrac{f_{2n}P_S + P_R}{1 + f_{2n}}, & (x < 0), \end{cases} \tag{4.8}$$

where

$$f_{2p}(x) = \left(\frac{K_{2R}}{K_{2S}}\right)^2 \left[\left(1 + \frac{x}{x_0}\right)\left(1 + k_{2S}\frac{x}{x_0}\right)\right]^2. \tag{4.9a}$$

$$f_{2n}(x) = \left(\frac{K_{2S}}{K_{2R}}\right)^2 \left[\left(1 - \frac{x}{x_0}\right)\left(1 - k_{2R}\frac{x}{x_0}\right)\right]^2. \tag{4.9b}$$

Substituting the pressure expressions (4.6) and (4.8) into the flow rate relations (4.4) and (4.5), we obtain the orifice flow relations

$$\begin{aligned} Q_{1S} &= Q_{1R} \\ &= \begin{cases} K_{1S}(P_S - P_R)^{1/2}(x_0 + x)(1 + f_{1p})^{-1/2}, & (x \geq 0), \\ K_{1R}(P_S - P_R)^{1/2}(x_0 - x)(1 + f_{1n})^{-1/2}, & (x < 0). \end{cases} \end{aligned} \tag{4.10a}$$

and

$$Q_{2S} = Q_{2R}$$
$$= \begin{cases} K_{2R}(P_S - P_R)^{1/2}(x_0 + x)(1 + f_{2p})^{-1/2}. & (x \geq 0). \\ K_{2S}(P_S - P_R)^{1/2}(x_0 - x)(1 + f_{2n})^{-1/2}. & (x < 0). \end{cases} \tag{4.10b}$$

for a servovalve with blocked control ports.

For a symmetric servovalve with matched control ports, we may write

$$K = K_{1S} = K_{1R} = K_{2S} = K_{2R}.$$
$$k = k_{1S} = k_{1R} = k_{2S} = k_{2R}.$$

so that we obtain

$$f_{1p} = f_{2p}.$$
$$f_{1n} = f_{2n}.$$

Since these relations associate the term $+x$ with positive spool displacements and $-x$ with negative spool displacements in Eqs. (4.7) and (4.9), they may be combined in a single expression $f(x)$ of the form

$$f(x) = \left(1 + \frac{|x|}{x_0}\right)^2 \left(1 + k\frac{|x|}{x_0}\right)^2.$$

which is valid for both $(x \geq 0)$ and $(x < 0)$.

Since the control ports are blocked for an internal leakage test, the total supply flow Q_S actually represents the internal leakage flow. Therefore, substituting (4.10) into (4.3), the internal leakage flow can be expressed as

$$Q_S(x) = 2K\,(P_S - P_R)^{1/2}\,(x_0 + |x|)\,(1 + f(x))^{-1/2}. \tag{4.11}$$

Hence we obtain an analytical expression of the total internal leakage flow in a servovalve as a function of spool position during an internal leakage test. Similarly, using pressure relations (4.6) and (4.8), an analytical relation for the load pressure ($P_L = P_1 - P_2$) can be expressed as

$$P_L(x) = \frac{f(x) - 1}{f(x) + 1} (P_S - P_R) \operatorname{sgn}(x). \tag{4.12}$$

which is valid during a pressure sensitivity test. Here $\operatorname{sgn}(\cdot)$ denotes the signum function. By comparing Eqs. (4.11) and (4.12) with the manufacturer's data, we may determine the unknown model parameters (K, x_0, k). In practice, we will substitute these parameters in servovalve model equations (4.4) and (4.5), which are valid regardless of the ports being blocked or unblocked.

4.4 Determination of Model Parameters

In this section we present a convenient method of determining the servovalve leakage parameters (K, x_0, k) from readily available manufacturer data for a symmetric servovalve with matched ports. The required data consists of the *rated* flow values, null leakage flow rate, and the pressure sensitivity curve at a given supply pressure. Later the estimated parameters are used to compare the model against experimental data at various supply pressures.

The rated (maximum) flow Q_{max} is the flow rate obtainable when the rated input current I_{max} is applied to the valve at a given valve pressure drop

$$P_V \doteq P_S - P_R - P_L.$$

Rated flow is usually specified for no-load condition ($P_L = 0$).

The maximum leakage flow, which occurs at neutral spool position, is only a few percent of the rated flow rate. In addition, the leakage flow rate decreases rapidly with valve stroke.

because spool lands overlap the valve orifices [38]. Hence, under rated flow conditions (Q_{max}, I_{max}) and no-load flow ($P_L = 0$) at servovalve ports, leakage flow terms in Eqs. (4.4) and (4.5) can be ignored. The result is the classical servovalve flow model at rated flow values [38]:

$$Q_{max} = \frac{K}{\sqrt{2}}(P_S - P_R)^{1/2} I_{max},$$

so that the flow gain K is given by

$$K = \frac{\sqrt{2} Q_{max}}{(P_S - P_R)^{1/2} I_{max}}. \tag{4.13}$$

The equivalent orifice opening x_0 is calculated using the leakage flow expression (4.11). The leakage flow rate at null is given by

$$Q_S(x = 0) = \sqrt{2} K (P_S - P_R)^{1/2} x_0,$$

so that we obtain

$$x_0 = \frac{Q_S(x = 0)}{\sqrt{2} K (P_S - P_R)^{1/2}}. \tag{4.14}$$

Finally, the leakage coefficient k can be obtained from the pressure sensitivity expression (4.12). The value of the pressure curve at $x = x_0$ is given by

$$P_L(x_0) = \frac{4(1+k)^2 - 1}{4(1+k)^2 + 1}(P_S - P_R). \tag{4.15}$$

Solving Eq. (4.15) for k, we obtain

$$k = \frac{1}{2}\sqrt{\frac{P_S - P_R + P_L(x_0)}{P_S - P_R - P_L(x_0)}} - 1. \tag{4.16}$$

Therefore, substituting manufacturer data for rated flow at rated current (Q_{max}, I_{max}), and

null leakage flow ($Q_S(x = 0)$) into Eqs. (4.13) and (4.14), and using the pressure sensitivity data in Eq. (4.16), we can determine the model parameters (K, x_0, k).

It is interesting to note that the allowed values of the parameter k ($0 < k < \infty$), when substituted into Eq. (4.15), result in $0.6\ (P_S - P_R) < P_L(x_0) < (P_S - P_R)$. A typical ordinate $P_L(x_0)$ is shown in Figure 4.3, where $P_L(x)$ approaches rapidly to its upper value $P_S - P_R$.

4.5 Model Evaluation

The servovalve model with leakage has been validated using a Moog 760-723A servovalve with 40 liter per minute no-load rated flow at 70 bar valve pressure drop and 25 mA rated current. The experimental servovalve data has been provided by Moog Inc. The details of leakage flow and pressure sensitivity tests are provided in [50]. The model parameters are calculated using servovalve data at $P_S = 137.9$ bar together with Eqs. (4.13), (4.14), and (4.16). The resulting parameters are as follows:

$$K = 1.46 \times 10^{-5}, \qquad x_0 = 8.28 \times 10^{-5}, \qquad k = 2.93 \times 10^{-1}.$$

Note that the same estimated parameters are used in subsequent simulations at various supply pressures. The simulated leakage flow curves are plotted together with the experimental results in Figure 4.5, where we used the above parameters in Eq. (4.11) for simulations. Similarly, the pressure sensitivity curves are generated using Eq. (4.12). These curves are plotted together with the experimental results in Figure 4.6.

A comparison of simulated and experimental results in Figs. 4.5 and 4.6 confirms the accuracy of the servovalve model in Eqs. (4.4) and (4.5). However, as seen in Figure 4.5, the leakage flow model in Eq. (4.11) slightly overestimates the leakage flow around the neutral spool position. Since we neglected the effect of leakage flow at rated flow conditions (Q_{max}, I_{max}) for parameter identification, Eq. (4.13) results in a slightly larger value of the flow gain K. As the parameter K is a multiplier in Eq. (4.11), a larger value shifts the leakage flow curve upwards, more at larger flow rates around null. However, note that the

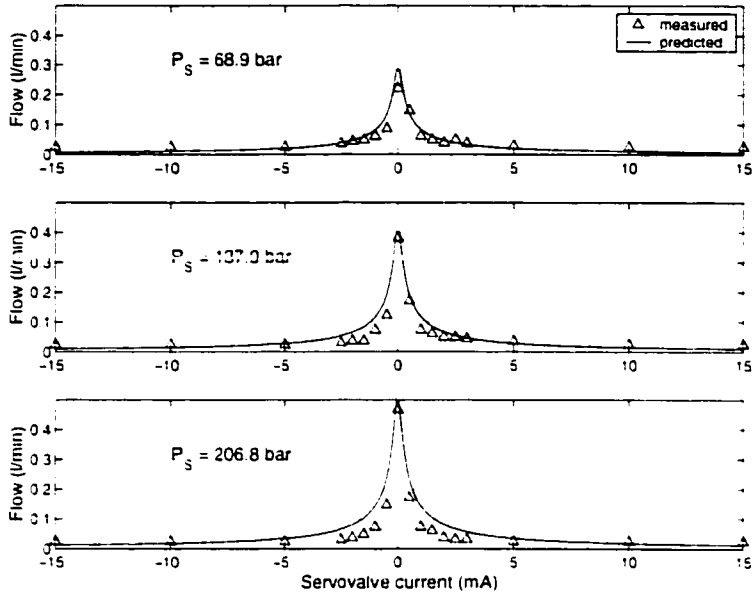

Figure 4.5: Leakage flow (Q_S): experiment and simulation.

parameter K does not appear in pressure sensitivity relation (4.12), so that the resulting curves in Figure 4.6 are not affected and remain accurate.

4.6 Conclusions

In this chapter, we present a nonlinear servovalve pressure-flow model that accurately captures servovalve leakage behavior. The leakage behavior is modeled as turbulent flow with a flow area inversely proportional to the overlap between the spool land and the servovalve orifices. The model only assumes a critical center spool, and is valid over the entire range of spool travel. In particular, at zero spool displacement, the expressions for *(a)* turbulent orifice flow for positive openings and *(b)* leakage flow due to spool-valve overlap predict identical flows. This produces a continuous flow relation.

The validity of the model is demonstrated by comparing experimental and simulated behavior of a servovalve. The model parameters are calculated using manufacturer data. It is shown that the model can accurately predict the leakage performance of a servovalve for

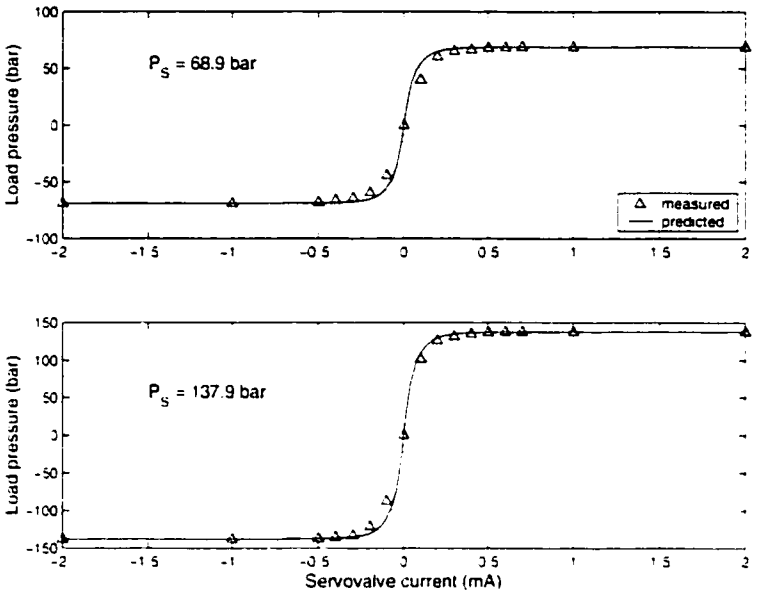

Figure 4.6: Load pressure (P_L): experiment and simulation.

different values of operating pressures.

The model developed may form the basis for improved control design. By using this leakage model, a designer can take advantage of nonlinear control techniques to achieve further improvements in servovalve and hydraulic system performance. Especially in applications that require precise actuator positioning, existing nonlinear controllers may be redesigned to accommodate additional nonlinearities due to servovalve leakage.

Chapter 5

Improved Control of Hydraulic Systems using Singular Perturbation Theory

5.1 Introduction

The dynamics of hydraulic systems involve slow and fast modes. These modes are associated with the mechanical components and components involving fluid flow, respectively. As such, controllers for hydraulic systems can be designed and analyzed using the tools of singular perturbation theory. A large body of results on singularly perturbed systems exist in the control literature, and these results have been successfully applied to feedback design of nonlinear systems [33, 34, 35]. However there exist few applications of singular perturbation methods to hydraulic control systems. Kim [32] uses singular perturbation techniques to improve spool positioning of a servovalve in an active car suspension application. The resulting feedback system, based on a first order approximation of the servovalve spool dynamics, is equivalent to a high gain control system.

In this investigation, we consider control of the hydraulic system in Figure 5.1. The spool position, x_v, is the input. As internal servovalve dynamics are often sufficiently fast

so as to be ignored in a model. this is a reasonable choice as the controlled input. The piston position. x_p. is the output. The system in Figure 5.1 is representative of many manufactur-

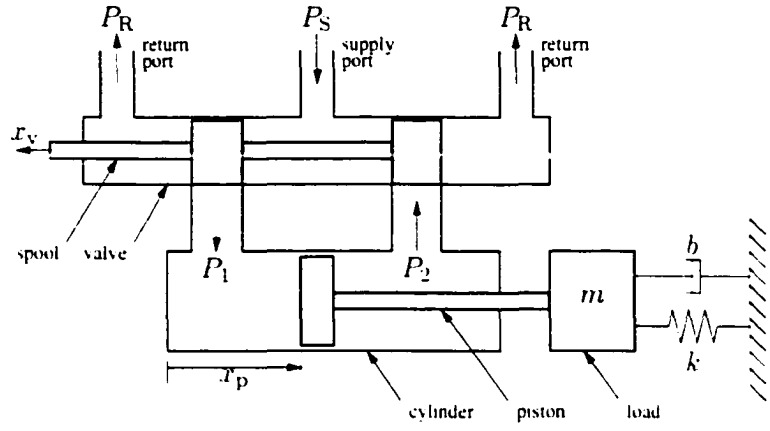

Figure 5.1: A generic hydraulic system configuration.

ing systems where the hydraulic piston drives a load with its own dynamics. For example. hydraulic material testing machines. machine tool drives. or robotic arms in contact with their environment all fit into this structure. Conventional controllers for these systems are usually designed using a simplified model in which the fast dynamics of the hydraulic system are ignored. However. this ad-hoc approach stems from practical convenience and lacks rigorous justification. An analytical study would help develop and evaluate high performance controllers for hydraulic systems. By bringing singular perturbation control techniques into the realm of hydraulic systems. it is possible to match model complexity with the control requirements. thus providing better performance.

Nonlinear control of hydraulic systems has attracted considerable attention in the past decade. Various nonlinear force and position control algorithms for hydraulic systems are developed in [6. 27. 45]: and applications of similar designs can be found in [7. 8. 40]. All of these designs include the effective bulk modulus. β. in the controller as a *known* and *fixed* parameter. However. in practice. bulk modulus is difficult to measure. Furthermore. due to temperature variations and air entrapment. the bulk modulus may vary during the operation of the hydraulic system.

Some existing controllers require what may be restrictive assumptions. In Alleyne [6], a nonlinear force tracking controller includes the effects of servovalve dynamics into the design. However, *(1)* the resulting controls require the derivative of the load pressure, $P_1 - P_2$, which may cause performance degradation due to the noisy nature of pressure measurements; and *(2)* the design assumes that cylinder chamber volumes are constant. To prevent performance degradation at large piston displacements, this assumption may necessitate a conservative design. In Sohl and Bobrow [45], nonlinear force and position tracking controllers are designed using Lyapunov-based analysis. They address the problem of variable chamber volumes by explicitly including the volume changes into the design. But, the design requires the derivative of the desired force, which in turn involves the piston acceleration, $\ddot{x}_p$. Hence, either differentiation of measured piston velocity, or an extra sensor is required. Furthermore, the leakage flow is not taken into account during the design. In high performance applications where low friction (hydrostatically balanced) cylinders are used, the leakage flow may be large.

In this chapter, we present a controller design method for high performance hydraulic control systems. The design is based on singular perturbation theory [31] and a nonlinear feedback approach that is similar to Lyapunov techniques. The resulting controller will

- achieve trajectory following with small error,
- be robust to variations in the hydraulic fluid bulk modulus,
- not require piston acceleration feedback,
- not require derivatives of cylinder chamber pressures.

The approach we develop will keep the position tracking error arbitrarily small and have the added advantages listed above.

This chapter is organized as follows. In Section 5.2 we develop a nonlinear model of the hydraulic system in Figure 5.1. A brief background on singular perturbation theory and an important result based on Tikhonov's theorem are presented in Section 5.3. The control law based on singular perturbation methods is developed in Section 5.4. In Section 5.5 we

simulate the performance of the proposed control algorithm. Conclusions and directions for future research are discussed in Section 5.6.

5.2 Hydraulic System Model

In applications, a hydraulic actuator is typically a double-acting hydraulic cylinder, as shown in Figure 5.2. The piston motion is obtained by modulating the oil flow into and out

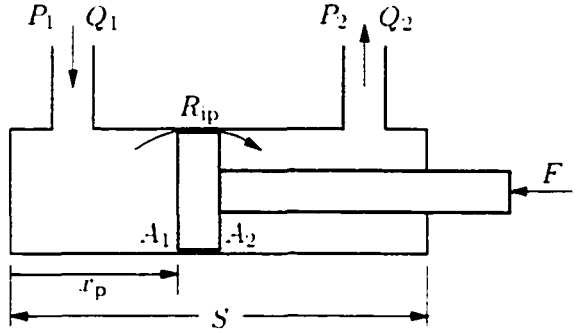

Figure 5.2: Double-acting hydraulic piston.

of the cylinder chambers, which are connected to a servovalve through cylinder ports. The servovalve provides this modulation. For a critically centered valve as shown in Figure 5.1, the flow rate equations can be expressed as

$$Q_1 = \begin{cases} \alpha \operatorname{sgn}(P_S - P_1)\,|P_S - P_1|^{1/2}\, x_v, & (x_v \geq 0) \\ \alpha \operatorname{sgn}(P_1 - P_R)\,|P_1 - P_R|^{1/2}\, x_v, & (x_v < 0), \end{cases}$$

and

$$Q_2 = \begin{cases} \alpha \operatorname{sgn}(P_2 - P_R)\,|P_2 - P_R|^{1/2}\, x_v, & (x_v \geq 0) \\ \alpha \operatorname{sgn}(P_S - P_2)\,|P_S - P_2|^{1/2}\, x_v, & (x_v < 0), \end{cases}$$

where $\alpha = C_d w \sqrt{2/\rho}$ and C_d is the discharge coefficient, w is the valve area gradient, and ρ is the fluid mass density [23, 45]. The application of the continuity equation to the two

sides of the cylinder yields

$$\frac{1}{\beta}\dot{P}_1 = \frac{1}{V_1}\left[-\dot{V}_1 - R_{ip}(P_1 - P_2) + Q_1\right]. \tag{5.1a}$$

$$\frac{1}{\beta}\dot{P}_2 = \frac{1}{V_2}\left[-\dot{V}_2 + R_{ip}(P_1 - P_2) - Q_2\right]. \tag{5.1b}$$

where

$$V_1 = V_{10} + A_1 x_p.$$

$$V_2 = V_{20} + A_2(S - x_p)$$

are the total fluid volumes in the two sides of the cylinder [38]. Here, S is the piston stroke, V_{10} and V_{20} are the fluid volumes in the lines between the cylinder and the servovalve, and R_{ip} is the internal leakage coefficient.

The actuator force due to the pressure differential across the piston is $F = A_1 P_1 - A_2 P_2$. Differentiating this expression and substituting the pressure equations (5.1) results in

$$\frac{1}{\beta}\dot{F} = f(x_p, \dot{x}_p, P_1, P_2) + g(x_p, P_1, P_2)\, x_v. \tag{5.2}$$

where

$$f = -\dot{x}_p\left[\frac{A_1^2}{V_1} + \frac{A_2^2}{V_2}\right] - R_{ip}(P_1 - P_2)\left[\frac{A_1}{V_1} + \frac{A_2}{V_2}\right]. \tag{5.3}$$

and

$$g = \begin{cases} \dfrac{A_1\alpha}{V_1}\operatorname{sgn}(P_S - P_1)\,|P_S - P_1|^{1/2} \\ \quad + \dfrac{A_2\alpha}{V_2}\operatorname{sgn}(P_2 - P_R)\,|P_2 - P_R|^{1/2}, \ (x_v \geq 0) \\ \dfrac{A_1\alpha}{V_1}\operatorname{sgn}(P_1 - P_R)\,|P_1 - P_R|^{1/2} \\ \quad + \dfrac{A_2\alpha}{V_2}\operatorname{sgn}(P_S - P_2)\,|P_S - P_2|^{1/2}, \ (x_v < 0). \end{cases} \tag{5.4}$$

An important feature of the above model is that the control input x_v appears *explicitly*

and *linearly* in the force equation (5.2). Hence the control input can be chosen to simplify the force equation to impose a desired form [45]. We also place the bulk modulus term on the left hand side of Eq. (5.2). This will help develop a control law based on singular perturbation theory, where the term $1/\beta$ acts as a perturbation parameter. Before developing this in Section 5.4, we provide a brief background on singularly perturbed systems.

5.3 Singularly Perturbed Systems

We will consider hydraulic systems modeled with the following standard full singular perturbation description:

$$\dot{x} = f(x, z, t), \quad x(0) = x_0, \tag{5.5a}$$

$$\varepsilon \dot{z} = g(x, z, t), \quad z(0) = z_0, \tag{5.5b}$$

where $x \in \mathbb{R}^n$ is the state of the slow subsystem, $z \in \mathbb{R}^m$ is the state of the fast subsystem, and $\varepsilon > 0$ is a small parameter. We use $x(t, \varepsilon)$ and $z(t, \varepsilon)$ to denote the solution of the full singular perturbation problem.

The key idea of singular perturbation control methods is to split the dynamics of the system into two separate time-scales, so that the resulting design problems are easier to solve than the design problem of the full singularly perturbed system. Two-time scale decomposition of Eqs. (5.5) can be done by setting $\varepsilon = 0$. In this case the dynamics of z become instantaneous and the two equations degenerate into the differential-algebraic equations

$$\dot{x} = f(x, z, t), \quad x(0) = x_0 \tag{5.6a}$$

$$0 = g(x, z, t) \tag{5.6b}$$

of order n. Assuming that it exists, let $z = h(x, t)$ be the unique isolated root of Eq. (5.6b) such that $g(x, h(x, t), t) = 0$ for all $x \in \mathbb{R}^n$ and $t \geq 0$. The *reduced-order* system is defined

as

$$\dot{x} = f(x, h(x,t), t), \quad x(0) = x_0. \tag{5.7}$$

Let $\bar{x}(t)$ be the solution of the reduced order system Eq. (5.7). The "quasi-steady-state" of z is then defined as $\bar{z}(t) = h(\bar{x}(t), t)$.

We define a new fast coordinate $y = z - h(x,t)$ and a fast time-scale $\tau = t/\varepsilon$ so that the singularly perturbed system (5.5) takes the form

$$\frac{dx}{d\tau} = \varepsilon f(x, y + h(x,t), t), \tag{5.8a}$$

$$\frac{dy}{d\tau} = g(x, y + h(x,t), t) - \varepsilon \frac{\partial h}{\partial t} - \varepsilon \frac{\partial h}{\partial x} f(x, y + h(x,t), t). \tag{5.8b}$$

in the (x, y) coordinates. Setting $\varepsilon = 0$ in Eqs. (5.8) results in the *boundary-layer* system

$$\frac{dy}{d\tau} = g(x, y + h(x,t), t), \quad y(0) = z_0 - h(x,t). \tag{5.9}$$

which has an equilibrium point at $y = 0$. Here the variables (x,t) are treated as constant parameters.

The response properties of the full singularly perturbed system (5.5) can be derived from the properties of the reduced-order (5.7) and the boundary-layer systems (5.9). In particular, under the assumptions of the Tikhonov's theorem (Appendix 5.7), it can be shown that there exist $t_1 > 0$ and $\varepsilon^* > 0$ such that

$$x(t, \varepsilon) - \bar{x}(t) = O(\varepsilon). \tag{5.10a}$$

$$z(t, \varepsilon) - h(\bar{x}(t), t) = O(\varepsilon). \tag{5.10b}$$

for $t \geq t_1$, whenever $\varepsilon < \varepsilon^*$. Here $O(\cdot)$ is the order of magnitude notation [31]. Hence, the theorem guarantees that following a boundary-layer transition for $t \in [0, t_1)$ the slow states of Eqs. (5.5) will remain close to the states of the reduced-order system and the fast states

will approach to their quasi-steady-state.

A mathematical model of the hydraulic system in Figure 5.1 can be expressed in the form of the singular perturbation description of Eqs. (5.5). Then, provided that a suitable control law can be developed, a closed-loop system can be designed such that the tracking error of the piston motion is kept small and the pressure transients are attenuated rapidly.

5.4 Control Law Design

The terms in Eqs. (5.3) and (5.4) consist of measured system states, $(x_p, \dot{x}_p, P_1, P_2)$, and of simple functions of known model parameters (e.g. $V_1 = V_{10} + A_1 x_p$). Therefore, for a given set of model parameters, the functions f and g can be computed online. Note that the variable and difficult-to-quantify fluid bulk modulus, β, is not a parameter in f or g, whereas the remaining terms are easily measured or computed.

The goal of the design is to modulate the piston force (F) to control the piston position (x_p) using the spool position input (x_v) to achieve this. To simplify the force equation (5.2), we select the spool position command to be of the form

$$x_v = \frac{1}{g}\left[-f - K(F - h(\cdot))\right]. \tag{5.11}$$

where K is a constant; and the function $h(\cdot)$ will be synthesized in such a manner that the piston follows a desired position profile. Substituting Eq. (5.11) in Eq. (5.2), we obtain

$$\varepsilon \dot{F} = -K(F - h), \quad \varepsilon = 1/\beta.$$

Then the equations of motion of the hydraulic system in Figure 5.1 can be expressed as

$$m\ddot{x}_p + b\dot{x}_p + kx_p = F, \tag{5.12a}$$

$$\varepsilon \dot{F} = -K(F - h). \tag{5.12b}$$

Given a smooth desired trajectory, $x_d(t)$, of the piston, we define the position tracking

error, $e(t)$, and the boundary-layer variable, $y(t)$, as

$$e = x_{\mathrm{p}} - x_{\mathrm{d}} \quad \text{and} \quad y = F - h,$$

where the function h is chosen such that

$$h(e, \dot{e}, t) = v(e, \dot{e}) + F_{\mathrm{d}}(t) \tag{5.13}$$

with

$$v(e, \dot{e}) = (b - mk_{\mathrm{v}})\dot{e} + (k - mk_{\mathrm{p}})e,$$
$$F_{\mathrm{d}} = m\ddot{x}_{\mathrm{d}} + b\dot{x}_{\mathrm{d}} + kx_{\mathrm{d}}.$$

Substituting Eq. (5.13) into Eqs. (5.12), the equations of motion of the hydraulic system in the new slow state variable, e, and the new fast state variable, y, become

$$m(\ddot{e} + k_{\mathrm{v}}\dot{e} + k_{\mathrm{p}}e) = y, \tag{5.14a}$$
$$\varepsilon\dot{y} = -Ky - \varepsilon\dot{h}. \tag{5.14b}$$

As $\varepsilon \to 0$, we obtain the reduced-order and boundary-layer systems in the new state variables expressed as

$$\ddot{e} + k_{\mathrm{v}}\dot{e} + k_{\mathrm{p}}e = 0, \tag{5.15a}$$
$$\frac{dy}{d\tau} = -Ky. \tag{5.15b}$$

for $m \neq 0$ and $\tau = t/\varepsilon$.

For positive values of the parameters k_{v}, k_{p}, and K, the equations (5.15) are globally exponentially stable with equilibrium points at $\bar{e} = \dot{\bar{e}} = y = 0$. In addition, selecting $h(e, \dot{e}, t)$ to have bounded first partial derivatives with respect to its arguments, we can

apply Theorem 5.7.1. The relations (5.10) yield

$$e(t,\varepsilon) - \overline{e}(t) = O(\varepsilon).$$
$$\dot{e}(t,\varepsilon) - \dot{\overline{e}}(t) = O(\varepsilon).$$
$$F(t,\varepsilon) - h(\overline{e}(t),t) = O(\varepsilon).$$

for all $t \geq t_1 > 0$. Since the exponentially stable slow system has equilibrium at the origin, we obtain

$$\lim_{t\to\infty} \overline{e}(t) = 0 \quad \Rightarrow \quad \lim_{t\to\infty} e(t,\varepsilon) = O(\varepsilon).$$

In particular, the choice of the function h as in Eq. (5.13) results in a closed-loop hydraulic system that will follow a given trajectory with small error. Similar arguments also yield

$$\lim_{t\to\infty} \dot{e}(t,\varepsilon) = O(\varepsilon).$$
$$\lim_{t\to\infty} [F(t,\varepsilon) - F_{\mathrm{d}}(t)] = O(\varepsilon).$$

Since the errors are of the order $O(\varepsilon) = O(1/\beta)$, it is clear that a system with sufficiently large bulk modulus will track a reference path with very small error. It should be noted that there exists a lower limit, β^*, of the bulk modulus such that if $\beta < \beta^*$, the hydraulic system tracking performance will degrade. However this lower limit is usually much less than the normal range of the bulk moduli encountered in practical applications. The closed-loop performance and robustness properties of the hydraulic system in Figure 5.1 are illustrated in the next section.

5.5 Controlled Hydraulic System Simulations

The control design consists of three parts. First, given a smooth trajectory, x_{d}, the control signal, x_{v}, in Eq. (5.11) is computed online using the measured states. The control signal

transforms the hydraulic system dynamics as expressed by Eqs. (5.14) in terms of the variables e and y. Since the perturbation parameter, ε, is sufficiently small by assumption, the hydraulic system dynamics are approximately described by Eq. (5.15). In particular, the tracking error dynamics are described by the differential equation (5.15a), which has a stable equilibrium at the origin for positive values of k_p and k_v. The second design step is to select the gains k_p and k_v to achieve fast error convergence to zero. We express these gains as

$$k_v = 2\zeta\omega_n \quad \text{and} \quad k_p = \omega_n^2. \tag{5.16}$$

and select $\zeta = \sqrt{2}/2$ to obtain a critically damped error dynamics. The variable ω_n provides a measure of the bandwidth of the error dynamics. Finally, the gain of the fast system is designed to obtain fast convergence of the boundary-layer variable y to zero. In general, a larger gain, K, provides faster convergence of the boundary-layer system, but too large a value may cause actuator saturation.

We performed various simulations to determine the controller's performance in providing position tracking. Model parameters used in simulations are

$$\begin{aligned} m &= 12 & b &= 20 & k &= 50 \times 10^3 \\ \omega_n &= 40\pi & \zeta &= 0.71 & K &= 1.0 \times 10^{-6} \\ \beta_{nom} &= 6.9 \times 10^8 \end{aligned}$$

in standard SI units.

The response of the hydraulic system to a 10 Hz sinusoidal trajectory input of 0.05 m amplitude is shown in Figure 5.3 for $\beta = \beta_{nom}$. The maximum and steady-state errors are shown in Figure 5.4 as a function of bulk modulus. The system becomes marginally stable at $0.091\beta_{nom}$. However, it can be seen that the system is robust to large variations in bulk modulus within the range of $[0.1, 3.0]\,\beta_{nom}$, and that the errors stay small in the vicinity of β_{nom}. Indeed by Theorem 5.7.1, robustness is guaranteed for $\beta \in [0.1, \infty)\,\beta_{nom}$.

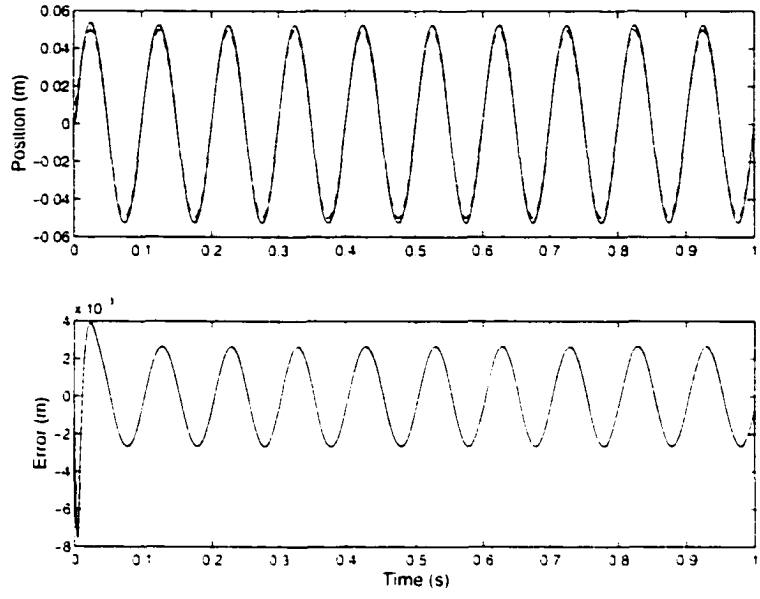

Figure 5.3: Tracking of a reference trajectory and tracking error (10 Hz sine).

The maximum and steady-state tracking errors converge to a constant value in Figure 5.4. As the bulk modulus becomes larger, we have $\varepsilon = 1/\beta \to 0$, so that the system dynamics are described by Eqs. (5.15). In the limit, the tracking error dynamics become independent of the fast transients, and are described by Eq. (5.15a). Therefore, the tracking error is limited by the choice of the parameters k_p and k_v, and in particular, by the choice of the error bandwidth through the relations (5.16).

We have also simulated the performance of the hydraulic system for a trajectory input with large displacements. The trajectory consists of steep ramps and large periodic motion throughout the range of the cylinder travel. The path is generated using Matlab's Spline Toolbox [15] and is smooth in the sense that its generating polynomials are twice continuously differentiable. Note that a smooth path is necessary to satisfy the differentiability requirements in the Tikhonov's theorem. The response of the hydraulic system for $\beta = \beta_{nom}$ is shown in Figure 5.5. The maximum errors as a function of bulk modulus are shown in Figure 5.6.

Unlike conventional and various nonlinear control designs, the tracking errors in our

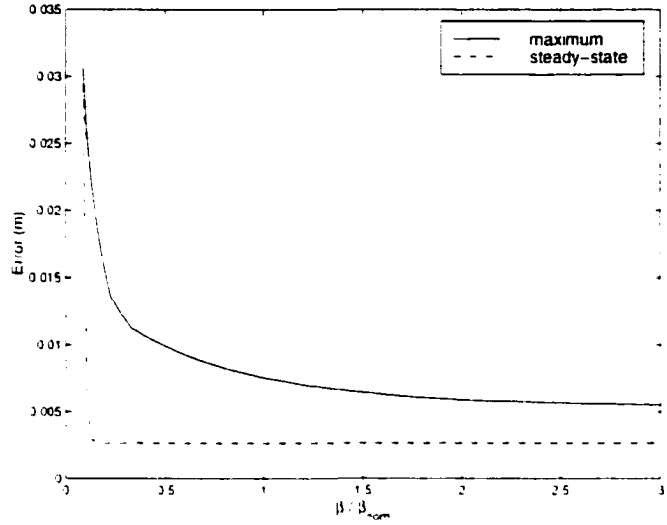

Figure 5.4: Maximum and steady-state errors as a function of bulk modulus (10 Hz sine).

design are small throughout the range of the cylinder stroke since the effects of variable cylinder chamber volumes are compensated for in the controller. In addition, it is also clear that the system preserves its robustness properties for large displacement inputs as well as high frequency small amplitude trajectories. In particular, since the time-variable bulk modulus is not a parameter in the controller, robustness is achieved without any computationally intense adaptive approach. Furthermore, improved tracking performance is obtained without the cost of additional sensors.

5.6 Conclusions

We have developed a design procedure for hydraulic control systems such that the resulting controller will

- achieve trajectory following with small error,
- be robust to variations in the hydraulic fluid bulk modulus,
- not require piston acceleration feedback,
- not require derivatives of cylinder chamber pressures.

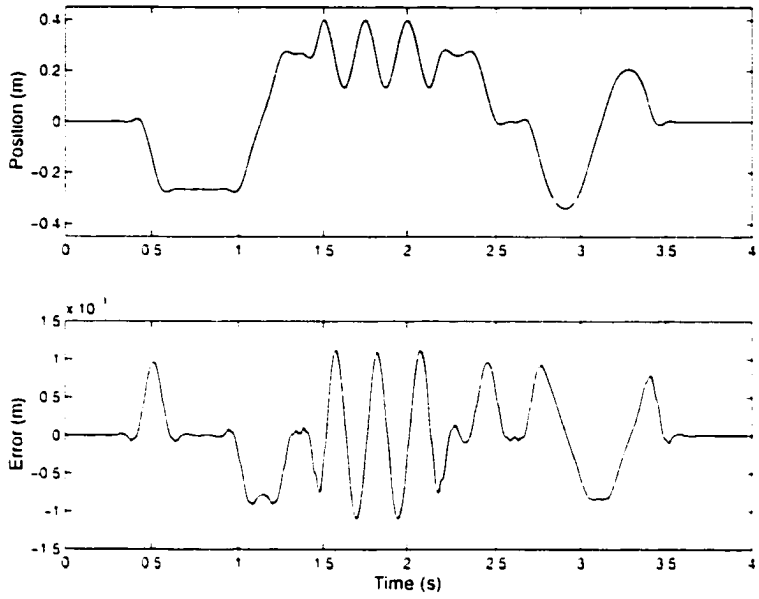

Figure 5.5: Tracking of a reference trajectory and tracking error (large displacement).

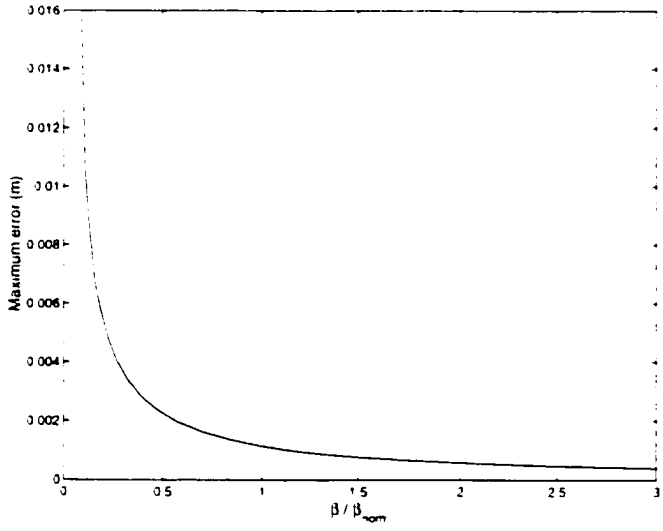

Figure 5.6: Maximum error as a function of bulk modulus (large displacement).

The design is based on the method of singular perturbation theory and a nonlinear feedback approach that uses Lyapunov techniques. Although our design will not achieve asymptotic command following, it will keep the position tracking error arbitrarily small and have the added advantages listed above. The authors also plan to validate the performance of this control design method on hardware in near future.

The control design approach adopted in this chapter improves on existing designs of hydraulic control systems in various aspects. The majority of these designs include the effective bulk modulus in the controller as a known and fixed parameter [40, 45]. In practice, bulk modulus may vary significantly due to temperature variations and air entrapment, which may result in loss of robustness of the hydraulic control system. In addition, many designs in the literature require the derivative of the load pressure, or the piston acceleration in the controller formulation [6, 45]. Furthermore, these designs may assume that cylinder chamber volumes are constant, which necessitates a conservative design [6, 7, 8]. Finally, in high performance applications where low friction cylinders are used, the leakage flow may be large, and it should be compensated in the design. All of these assumptions and requirements involve additional computations or additional sensors, and the resulting design may not provide robust performance. In contrast, the design provided in this chapter has none of the disadvantages described above.

Tikhonov's theorem guarantees that there is a range of parameters, $\varepsilon \in (0, \varepsilon^*)$, such that the full singularly perturbed system will track a given smooth trajectory with small error. However, exactly how small the tracking error will be, and the range of singular perturbation parameters for which Tikhonov's theorem hold, cannot be determined from the statement of the theorem. Our future work will address the problem of determining less conservative estimates of this range along the lines of the small-gain formulation, which looks promising in our work to date.

5.7 Appendix: Tikhonov's Theorem

We present a simplified global version of Tikhonov's theorem adapted from Khalil [31, pages 384-385]. In essence, the theorem states that for singularly perturbed systems with a sufficiently small perturbation parameter, if the fast and slow subsystems are exponentially stable, then the full system dynamics will be close to the dynamics of the reduced-order and boundary-layer systems, provided the initial conditions are sufficiently close to the origin.

Theorem 5.7.1. *Consider the singular perturbation problem* (5.5) *and let* $z = h(x,t)$ *be an isolated root of Eq.* (5.6b). *Assume that the following conditions are satisfied for all*

$$(x, z - h(x,t), t) \in \Re^n \times \Re^m \times [0, \infty).$$

- *The functions* f, g *and their first partial derivatives with respect to* x, z, t *are continuous and bounded. The function* $h(x,t)$ *has bounded first partial derivatives with respect to* x, t.
- *The Jacobian* $\partial g(x,z,t)/\partial z$ *and* $\partial f(x, h(x,t), t)/\partial x$ *have bounded first partial derivatives with respect to their arguments.*
- *The origin of the reduced-order system* (5.7) *is exponentially stable.*
- *The origin of the boundary-layer system* (5.9) *is exponentially stable, uniformly in* x, t.

Then, there exist positive constants c_1, c_2 *and* ε^* *such that for all*

$$\|x_0\| < c_1, \quad \|z_0 - h(x_0, 0)\| < c_2 \quad \text{and} \quad 0 < \varepsilon < \varepsilon^*,$$

the singular perturbation problem (5.5) *has a unique solution* $x(t,\varepsilon)$, $z(t,\varepsilon)$ *defined for all*

$t \geq 0$. *Moreover, given any* $t_1 > 0$, *we have*

$$x(t, \varepsilon) - \overline{x}(t) = O(\varepsilon). \tag{5.17}$$

$$z(t, \varepsilon) - h(\overline{x}(t), t) = O(\varepsilon). \tag{5.18}$$

for $t \geq t_1$ *whenever* $\varepsilon < \varepsilon^*$.

Chapter 6

Conclusions and Future Research

6.1 Contributions

Unified Valve Model. In Chapter 2, we developed a unified model for proportional control valves and analyzed the effect of spool lapping on open-loop hydraulic system properties [23]. The nonlinear mathematical equations relate the flow rates through the valve ports to the valve parameters. The flow rates are expressed as a continuous but nonlinear function of *lapping parameters*, as well as other conventional parameters. These equations are readily applicable to various types of proportional valves, and they unify the cases of critical center, overlapped, and underlapped valves.

The spool lands' geometry are individually controlled via model parameters. An offset between the lands, and asymmetric neutral spool position can also be simulated using our model. The system model is fully implemented in Matlab's Simulink simulation package and the hydraulic system component models are combined in a library for easy reuse.

We also derived simplified flow rate equations under certain widely-used assumptions while keeping nonlinearities due to spool geometry. The variation of the flow gain and uncertainty bounds of the flow rates of an underlapped valve are also analyzed.

Although we assumed a constant bulk modulus, changes in temperature, pressure, and percent air in the fluid will alter this parameter. The assumption facilitated the analysis,

in particular the piecewise-linear characterization of flow versus spool displacement. If operating conditions are such that this assumption is invalid, adaptive [40] and singular perturbation [22] control approaches are available to accommodate the variation in bulk modulus.

Unified Model Accuracy. In Chapter 3, we analyzed the accuracy of the unified proportional valve model developed in Chapter 2. As suggested by a second-order linear model of a generic hydraulic system configuration, a non-dimensional analysis of the unified model confirms that the accuracy of the model is independent of the choice of a particular set of model parameters. In fact, for a given value of the hydraulic damping coefficient, the simulations of the model error do not depend on the model parameter values, as long as their combination results in a fixed damping coefficient. Therefore, the accuracy of the model can be determined a priori using similar simulations as described in the chapter. This would provide great flexibility to an engineer in deciding whether the unified model can be used for subsequent analysis and control design without introducing modeling errors due to the presence of valve dynamics.

It is also shown that the errors in using the unified valve model are less than 10 percent for frequencies up to one third of the natural frequency of the hydraulic system. Since most hydraulic systems are rarely driven above this frequency range, it has been concluded that the unified valve model provides an accurate representation of the valve dynamics for most applications.

Leakage Flow Model. In Chapter 4, we presented a nonlinear servovalve pressure-flow model that accurately captures servovalve leakage behavior [24, 25]. The leakage behavior is modeled as turbulent flow with a flow area inversely proportional to the overlap between the spool land and the servovalve orifices. The model only assumes a critical center spool, and is valid over the entire range of spool travel. In particular, at zero spool displacement, the expressions for *(a)* turbulent orifice flow for positive openings and *(b)* leakage flow due to spool-valve overlap predict identical flows. This produces a continuous flow relation.

The validity of the model is demonstrated by comparing experimental and simulated

behavior of a servovalve. The model parameters are calculated using manufacturer data. We have shown that the model can accurately predict the leakage performance of a servovalve for different values of operating pressures.

Singular Perturbation Control. In Chapter 5, we developed a design procedure for hydraulic control systems [22] such that the resulting controller will

- achieve trajectory following with small error.
- be robust to variations in the hydraulic fluid bulk modulus.
- not require piston acceleration feedback.
- not require derivatives of cylinder chamber pressures.

The design is based on the method of singular perturbation theory and a nonlinear feedback approach that uses Lyapunov techniques. Although our design will not achieve asymptotic command following, it will keep the position tracking error arbitrarily small and have the added advantages listed above.

The control design approach adopted in this chapter improves on existing designs of hydraulic control systems in various aspects. The majority of these designs include the effective bulk modulus in the controller as a known and fixed parameter [40, 45]. In practice, bulk modulus may vary significantly due to temperature variations and air entrapment, which may result in loss of robustness of the hydraulic control system. In addition, many designs in the literature require the derivative of the load pressure, or the piston acceleration in the controller formulation [6, 45]. Furthermore, these designs may assume that cylinder chamber volumes are constant, which necessitates a conservative design [6, 7, 8]. Finally, in high performance applications where low friction cylinders are used, the leakage flow may be large, and it should be compensated in the design. All of these assumptions and requirements involve additional computations or additional sensors, and the resulting design may not provide robust performance. In contrast, the design provided in this chapter has none of the disadvantages described above.

Summary of Publications. The results reported in this thesis have been published or submitted for publication in various journals and conference proceedings:

1. Bora Eryilmaz and Bruce H. Wilson. Improved control of hydraulic systems using singular perturbation theory. *ASME Journal of Dynamic Systems, Measurement, and Control.* 1999. In review.

2. Bora Eryilmaz and Bruce H. Wilson. Combining leakage and orifice flows in a hydraulic servovalve model. *Journal of Dynamic Systems, Measurement, and Control.* September 2000. To be published.

3. Bora Eryilmaz and Bruce H. Wilson. Modeling the internal leakage of hydraulic servovalves. In *Proceedings of the ASME Dynamic Systems and Control Division.* November 2000. To be published.

4. Bora Eryilmaz and Bruce H. Wilson. A unified model of a proportional valve. In Sanjay I. Mistry and Timothy McLain, editors, *Proceedings of the ASME Fluid Power Systems and Technology Division.* FPST-Vol. 6, pages 95–102, Nashville, TN, 1999. ASME International Mechanical Engineering Congress and Exposition.

6.2 Future Research

Our work to date provides a good foundation for further research in improving the performance of electrohydraulic systems. In particular, our results provide a basis for further developments in incorporating our proportional and servo valve models with various nonlinear control techniques and analyzing the robustness of these techniques to parameter variations. The design of nonlinear controllers for overlapped and underlapped valves is another a promising research area. Simple nonlinear compensators together with less expensive proportional valves may, in fact, offer substantial cost savings in hydraulic control systems design.

The leakage model developed may form the basis for improved control design. By using this leakage model, a designer can take advantage of nonlinear control techniques to achieve further improvements in servovalve and hydraulic system performance. Especially

in applications that require precise actuator positioning, existing nonlinear controllers may be redesigned to accommodate additional nonlinearities due to servovalve leakage.

In the design of our singular perturbation based controller, Tikhonov's theorem guarantees a range of perturbation parameters such that the full singularly perturbed system will track a given smooth trajectory with small error. However, exactly how small the tracking error will be, and the range of singular perturbation parameters for which Tikhonov's theorem hold, cannot be determined from the statement of the theorem. Future work should address the problem of determining less conservative estimates of this range. Our work to date suggests that the small-gain formulation may be a suitable approach.

In addition, our research provides new tools to analyze and improve the performance of electrohydraulic control systems. Possible applications of our results include the use of less expensive (and non-smooth nonlinear) proportional valves together with a nonlinear controller in active vehicle vibration isolation, where the valve cost is a major deterrent for commercial applications. In hydraulic material testing machines, the use of our leakage model may be used to improve the precision motion performance in some tests such as creep loading, where the valve spool mostly resides within the null region with relatively large leakage flows.

Bibliography

[1] *Proceedings of the 1995 American Control Conference*. Seattle, WA. June 1995.

[2] *Proceedings of the 1997 American Control Conference*. Albuquerque, New Mexico. June 1997.

[3] *Proceedings of the ASME Fluid Power Systems and Technology Division*. November 1997. ASME International Mechanical Engineering Congress and Exposition.

[4] *Proceedings of the 1998 American Control Conference*. Philadelphia, PA. June 1998.

[5] *Proceedings of the ASME Fluid Power Systems and Technology Division*. Anaheim, CA. November 1998. ASME International Mechanical Engineering Congress and Exposition.

[6] Andrew Alleyne. Nonlinear force control of an electro-hydraulic actuator. In *Japan-USA Symposium on Flexible Automation*, pages 193–200. Boston, MA. June 1996. American Society of Mechanical Engineers.

[7] Andrew Alleyne and J. Karl Hedrick. Nonlinear control of a quarter car active suspension. In *Proceedings of the 1992 American Control Conference*, pages 21–25. Chicago, IL. June 1992.

[8] Andrew Alleyne and J. Karl Hedrick. Nonlinear adaptive control of active suspensions. *IEEE Transactions on Control Systems Technology*, 3(1):94–101. March 1995.

[9] Andrew Alleyne, Rui Liu, and Heather Wright. On the limitations of force tracking control for hydraulic active suspensions. In *Proceedings of the 1998 American Control Conference* [4], pages 43–47.

[10] Wayne R. Anderson. *Controlling Electrohydraulic Systems*. Marcel Dekker, New York, NY, 1988.

[11] B. W. Barnard and P. Dransfield. Predicting response of a proposed hydraulic control system using bond graphs. *ASME Journal of Dynamic Systems, Measurement, and Control*, pages 1–8, March 1977.

[12] J. E. Bobrow and K. Lum. Adaptive, high bandwidth control of a hydraulic actuator. In *Proceedings of the 1995 American Control Conference* [1], pages 71–75.

[13] C.-C. Chen. Global exponential stabilisation for nonlinear singularly perturbed systems. *IEE Proc.-Control Theory Applications*, 145(4):377–382, 1998.

[14] B. d'Andréa Novel, M.A. Garnero, and A. Abichou. Nonlinear control of a hydraulic robot using singular perturbations. In *Proceedings of the IEEE International Conference on Systems, Man and Cybernetics*, pages 1932–1937, 1994.

[15] Carl de Boor. *Matlab Spline Toolbox*. The MathWorks, Natick, MA, December 1997.

[16] Stephen R. H. Dean, Brian W. Surgenor, and Harry N. Iordanou. Experimental evaluation of a backlash inverter as applied to a servomotor with gear train. In Joe Chow and Dean Minto, editors, *Proceedings of the 4th IEEE Conference on Control Applications*, pages 580–583, Albany, NY, September 1995.

[17] P. Dransfield and M. K. Teo. Using bond graphs in simulating an electro-hydraulic system. *Journal of The Franklin Institute*, 308(3):173–184, 1979.

[18] Asko Ellman. Leakage behaviour of four-way servovalve. In *Proceedings of the ASME Fluid Power Systems and Technology Division* [5], pages 163–167. ASME International Mechanical Engineering Congress and Exposition.

[19] Asko Ellman, K. Koskinen, and M. Vilenius. Through-flow in short annulus of fine clearance. In T. E. Alberts, editor, *Proceedings of the ASME Dynamic Systems and Control Division*, volume DSC-Vol. 57-2, pages 813–821, San Francisco, CA, November 1995. ASME International Mechanical Engineering Congress and Exposition.

[20] Asko Ellman and Tapio Virvalo. Formation of pressure gain in hydraulic servovalves and its significance in system behavior. In *Proceedings of the ASME Fluid Power Systems and Technology Division*, volume FPST-Vol. 3, pages 77–81, Atlanta, GA, November 1996. ASME International Mechanical Engineering Congress and Exposition.

[21] G. H. Engelman and G. Rizzoni. Including the force generation process in active suspension control formulation. In *Proceedings of the 1993 American Control Conference*, pages 701–705, San Francisco, CA, June 1993.

[22] Bora Eryilmaz and Bruce H. Wilson. Improved control of hydraulic systems using singular perturbation theory. *ASME Journal of Dynamic Systems, Measurement, and Control*, 1999. In review.

[23] Bora Eryilmaz and Bruce H. Wilson. A unified model of a proportional valve. In Sanjay I. Mistry and Tim McLain, editors, *Proceedings of the ASME Fluid Power Systems and Technology Division*, volume FPST-Vol. 6, pages 95–102, Nashville, TN, November 1999. ASME International Mechanical Engineering Congress and Exposition.

[24] Bora Eryilmaz and Bruce H. Wilson. Combining leakage and orifice flows in a hydraulic servovalve model. *ASME Journal of Dynamic Systems, Measurement, and Control*, 2000. To be published.

[25] Bora Eryilmaz and Bruce H. Wilson. Modeling the internal leakage of hydraulic servovalves. In *Proceedings of the ASME Dynamic Systems and Control Division*, November 2000. To be published.

[26] J. B. Gamble and N. D. Vaughan. Comparison of sliding mode control with state feedback and PID control applied to a proportional solenoid valve. *ASME Journal of Dynamic Systems. Measurement. and Control.* 118:434-438. September 1996.

[27] H. Hahn. A. Piepenbrink. and K.-D. Leimbach. Input/output linearization control of an electro servo-hydraulic actuator. In *Proceedings of the 1994 Conference on Control Applications.* pages 995–1000. Glasgow. UK. August 1994.

[28] H. M. Handroos and M. J. Vilenius. Flexible semi-emprical models for hydraulic flow control valves. *ASME Journal of Mechanical Design.* 113:232 238. September 1991.

[29] Cem Hatipoğlu and Ümit Özgüner. Robust control of systems involving non-smooth nonlinearities using modified sliding manifolds. In *Proceedings of the 1998 American Control Conference* [4]. pages 2133 2137.

[30] H. K. Khalil and Y. N. Hu. Steering control of singularly perturbed systems: A composite control approach. *Automatica.* 25:65 75. 1989.

[31] Hassan K. Khalil. *Nonlinear Systems.* Prentice-Hall. New York. NY. 1996.

[32] Eung-Seok Kim. Nonlinear indirect adaptive control of a quarter car active suspension. In *Proceedings of the 1996 Conference on Control Applications.* pages 61 66. Dearborn. MI. September 1996.

[33] P. V. Kokotović and H K. Khalil. editors. *Singular Perturbations in Systems and Control.* IEEE Press. New York. NY. 1986.

[34] P. V. Kokotović. H. K. Khalil. and J. O'Reilly. *Singular Perturbation Methods in Control: Analysis and Design.* Academic Press. New York. NY. 1986.

[35] Petar V. Kokotović. Applications of singular perturbation techniques to control problems. *SIAM Review.* 26(4):501–550. 1984.

[36] D. L. Margolis and C. Hennings. Stability of hydraulic motion control systems. *ASME Journal of Dynamic Systems. Measurement. and Control.* 119:605–613. December 1997.

[37] D. McCloy and H. R. Martin. *Control of Fluid Power: Analysis and Design.* Ellis Horwood. England. second edition. 1980.

[38] Herbert E. Merritt. *Hydraulic Control Systems.* John Wiley & Sons. New York. NY. 1967.

[39] D. P. Newell. H. Dai. M. K. Sain. P. Quast. and B. F. Spencer. Nonlinear modeling and control of a hydraulic seismic simulator. In *Proceedings of the 1995 American Control Conference* [1]. pages 801-805.

[40] H. J. Park. H. S. Cho. and B. S. Hyun. An adaptive control of nonlinear time-varying hydraulic servo systems. In *Proceedings of the 1989 American Control Conference.* pages 1894-1898. Pittsburgh. PA. June 1989.

[41] Darrel A. Recker. *Adaptive Control of Systems Containing Piecewise Linear Nonlinearities.* PhD thesis. University of Illinois at Urbana-Champaign. Urbana. IL. 1993.

[42] A. Saberi and H. K. Khalil. Stabilization and regulation of nonlinear singularly perturbed systems: Composite control. *IEEE Transactions on Automatic Control.* 30:739 747. 1985.

[43] P. M. Sharkey and J. O'Reilly. Composite control of nonlinear singularly perturbed systems: A geometric approach. *International Journal of Control.* 48(6):2491 2506. 1988.

[44] Garett A. Sohl and James E. Bobrow. Experiments and simulations on the nonlinear control of a hydraulic servosystem. In *Proceedings of the 1997 American Control Conference* [2]. pages 631-635.

[45] Garett A. Sohl and James E. Bobrow. Experiments and simulations on the nonlinear control of a hydraulic servosystem. *IEEE Transactions on Control Systems Technology.* 7(2):238–247. 1999.

[46] Gang Tao. Adaptive compensation for actuator imperfections. In *Proceedings of the 1997 American Control Conference* [2]. pages 3788–3792.

[47] Gang Tao and Petar V. Kokotović. Adaptive control of plants with unknown dead-zones. *IEEE Transactions on Automatic Control*. AC-39(1):59–68. 1994.

[48] Gang Tao and Petar V. Kokotović. Adaptive control of plants with unknown hystereses. *IEEE Transactions on Automatic Control*. AC-40(2):200–212. 1995.

[49] Gang Tao and Petar V. Kokotović. *Adaptive Control of Systems with Actuator and Sensor Nonlinearities*. John Wiley & Sons. New York. NY. 1996.

[50] William J. Thayer. Specification standards for electrohydraulic flow control servovalves. Technical Report 117. Moog Inc.. 1962.

[51] Gert-Wim van der Linden and Peter Valk. Digital control of an experimental hydraulic manipulator. In *Proceedings of the 1994 American Control Conference*. pages 2455 2459. Baltimore. MD. June 1994.

[52] N. D. Vaughan and J. B. Gamble. The modeling and simulation of a proportional solenoid valve. *ASME Journal of Dynamic Systems, Measurement, and Control*. 118:120–125. March 1996.

[53] R. B. Walters. *Hydraulic and Electro-Hydraulic Control Systems*. Elsevier Science. New York. NY. 1991.

[54] D. Wang. R. Dolid. M. Donath. and J. Albright. Development and verification of two-stage flow control servovalve model. In *Proceedings of the ASME Fluid Power Systems and Technology Division*. volume FPST-Vol. 2. pages 121–129. San Francisco. CA. November 1995. ASME International Mechanical Engineering Congress and Exposition.

[55] Heather Wright. Andrew Alleyne. and Rui Liu. On the stability and performance of two-stage hydraulic servovalves. In *Proceedings of the ASME Fluid Power Systems and*

Technology Division [3]. pages 215–222. ASME International Mechanical Engineering Congress and Exposition.

[56] Bin Yao. George T.-C. Chiu. and John T. Reedy. Nonlinear adaptive robust control of one-DOF electro-hydraulic servo systems. In *Proceedings of the ASME Fluid Power Systems and Technology Division* [2]. pages 191–197. ASME International Mechanical Engineering Congress and Exposition.

[57] Danian Zheng. Heather Havlicsek. and Andrew Alleyne. Nonlinear adaptive learning for electrohydraulic control systems. In *Proceedings of the ASME Fluid Power Systems and Technology Division* [5]. pages 83–90. ASME International Mechanical Engineering Congress and Exposition.